MP2 and DFT Analysis of the Ligand Selectivity of a Sulfotransferase Enzyme: SULT1A3

Diana Bigler

Department of Chemistry

Rhodes College

Memphis, Tennessee

2015

Submitted in partial fulfillment of the requirements for the

Bachelor of Science degree with Honors in Chemistry

This Honors paper by Diana Bigler has been read and approved for Honors in Chemistry.

Dr. Mauricio Cafiero

Project Advisor

_____

Dr. Larryn Peterson

Second Reader

_____

Dr. Erin Bodine

Extra-Departmental Reader

_____

Dr. Mauricio Cafiero

Department Chair

_____

ACKNOWLEDGEMENTS

First, I would like to express my gratitude to Dr. Cafiero, my research advisor, for all of the opportunities and support that he has provided to me.

I would like to thank Dr. Peterson for her time and advice throughout this process.

Also, thank you to the members of my research group and those of Dr. Peterson's research group.

I would also like to acknowledge the National Science Foundation for providing the computational resources that were necessary to complete this project.

CONTENTS

ABSTRACT

MP2 and DFT Analysis of the Ligand Selectivity of a Sulfotransferase Enzyme: SULT1A3
By
Diana Bigler

Sulfotransferase 1A3 (SULT1A3) helps regulate various endogenous and exogenous substrates in the body via sulfation. Dopamine and acetaminophen, for example, are known to be selectively sulfated in a reaction catalyzed by this enzyme. In order to characterize the selectivity of this enzyme, the electronic interaction energies between the SULT1A3 active site and eight dopaminergic ligands, two other structurally similar ligands, and resveratrol have been calculated using MP2 and M062X with the 6-311+G* basis set. The SULT1A3 active site was isolated from the crystal structure with dopamine bound (PBD ID: 2A3R). Structures for eleven ligands bound in the active site were obtained by three different optimization approaches with M062X/6-31G: by optimization *in vacuo* with rigid amino acid side chains where the ligand and protons were optimized; with implicit solvation by water with rigid amino acid side chains; and with implicit solvation by water and relaxed amino acid side chains. Calculations indicate that use of implicit solvent and a relaxed active site offer notable improvement in ligand interaction energies through stronger binding energies. The solvated-relaxed model shows less variability in ligand interaction than the other two models. Further, the influence of point mutations on the selectivity of SULT1A3 was investigated for dopamine, two dopamine analogues, and resveratrol using the solvated-relaxed model. Theoretical results here agree well with published experimental results. Finally, the interaction energy the SULT1A3 active site with salbutamol, a pharmaceutical and feed additive, was investigated, also using the solvated-relaxed model.

I give permission for public access to my Honors paper and for any copying or digitization to be done at the discretion of the College Archivist and/or the College Librarian.

Signed_____

Diana Bigler

Date _____

1. Introduction

1.1 **SULT1A3**

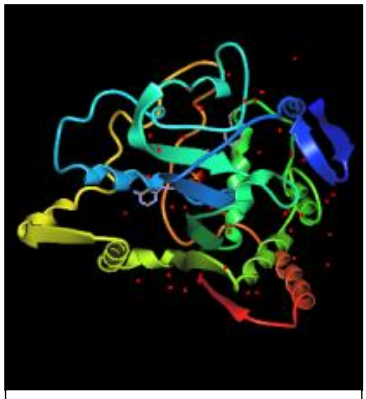

Figure 1. Crystal Structure of sulfotransferase SULT 1A3 with dopamine.

Sulfotransferases (SULTs), a supergene family composed of diverse enzymes, are involved in the regulation and metabolism of many xenobiotics, drugs, and other compounds within the human body. [1] The catalytic transfer of a sulfuryl moiety ($SO3^-$) from 3'-phosphoadenosine-5'-phosphosulfate (PAPS) to a hydroxyl or amino group on the ligand has a well-known mechanism as shown in the review by Gamage, *et al*.[1] A histidine residue, Histidine108, is highly conserved and is present in the active site of every sulfotransferase; it is responsible for the formation of hydrogen bond interactions to and the abstraction of the proton from the hydroxyl substituent group on the ligand.[2,3] Lysine106 also is involved in the formation of a hydrogen bond with the hydroxyl group on the ligand which helps to stabilize the bound ligand.[3]

When sulfated, most xenobiotics and other small substrates become more polar and thus water-soluble, allowing for excretion from the body or movement across cellular membranes.[1] Thus, knowledge of sulfotransferases is crucial pharmacology and drug design.

There are three families of sulfotransferase enzymes found in humans—SULT1, SULT2, and SULT4.[1] SULT1A is a subfamily of cytosolic sulfotransferases[4] that share high homology but show differing substrate preferences for phenolic ligands.[5] The current study focuses on one specific enzyme within this subfamily—SULT1A3 (Figure 1).

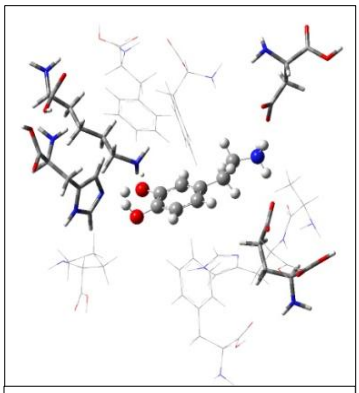

Figure 2. His108, Lys106, Glu146, Asp86 (right to left in cylinder frame) within SULT1A3 with optimized dopamine. Less significant residues are in wire frame.

A comparison of SULT1A3 with another member of the SULT1A category, SULT1A1, is helpful to understanding the types of ligands sulfated by each enzyme. Although SULT1A3 and SULT1A1 have ninety-three percent of the same sequence identity, they exhibit very different substrate specificity.[6] SULT1A3 shows preference toward charged substrates such as dopamine while SULT1A1 favors uncharged phenolic structures, such as *p*-nitrophenol (*p*Np).[3] Within the SULT1A3 active site, in addition to the His108 and Lys106 residues, the presence of the glutamic acid and aspartic acid residues at the 146 and 89 positions create an environment that is more favorable for charged molecules (Figure 2).[3] In comparison, the active site of SULT1A1 contains fewer charged amino acid residues, which explains the more favorable interactions of hydrophobic structures such as *p*Np.[3]

The sulfotransferases 1A1 and 1A3 are suspected to play a role in the regulation and metabolism of xenobiotics and neurotransmitters that enter the fetal circulation.[7] After the baby is born, the levels of SULT1A1 increase in the liver, while the levels of SULT1A3 drop off almost completely.[7] Levels of SULT1A3 in adults in hepatic tissue are small as compared to the levels of SULT1A1 and 1A2; SULT1A3 is most present in the jejunum, intestine, and the brain.[1] In the brain, SULT1A3 is located within the cytoplasm of the neuronal cells and is responsible for the sulfation of dopamine into the inactive sulfated-dopamine form.[8] This inactive form of dopamine accounts for over ninety percent of dopamine that is in circulation or in the cerebrospinal fluid within the body.[8] Because SULT1A3 is found only in humans and primates, but not in lower order

animals, the presence of this enzyme may be correlated to the evolutionary increase in the presence of catecholamines within these species.[8] Inhibition of SULT1A3 by pharmacological efforts results in an increase in dopamine toxicity within the cell.[8] This enzyme is responsible for the protection of neural cells from toxic levels of dopamine and is thus a target for investigating causes of neurodegenerative diseases.[8] It is thought that the three enzymes that metabolize dopamine—monoamine oxidase, catechol *O*-methyltransferase, and sulfotransferase SULT1A3—may have interdependent reactions for the metabolism of dopamine as well as other catecholamines.[8]

Catecholamines like dopamine, as well as other possible ligands of SULT1A3, can be sulfated at more than one position. Because dopamine has two hydroxyl groups, there are two possible products—dopamine-3-*O*- sulfate and dopamine-4-*O*-sulfate as illustrated in Figure 3.[9] The use of high-performance liquid chromatography can be used to distinguish between the two products.[9] In a study by Itäaho, *et al,* an enzyme kinetic analysis was performed to determine the major sulfated product, which was found to be dopamine-3-*O*-sulfate.[9] Other studies have found that this specific regioisomer of dopamine is the major form found in plasma in ten times the quantity of dopamine-4-*O*-sulfate.[10] The apparent K_m is reported to be comparable for both dopamine products; however, the V_{max} shows favor for sulfation at the hydroxyl group at the third position.[9] Studies have investigated the underlying cause for the selectivity of the SULT1A3 active site;[2,7] in a study by Strobel, *et al.*, it was suggested that it may not be the specificity of

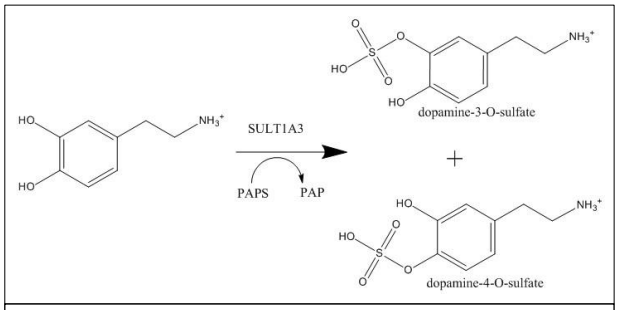

Figure 3. Sulfation of dopamine catalyzed by SULT1A3.

the sulfotransferase but rather the arylsulfatases or transport proteins that lead to the majority of dopamine-3-*O*-sulfate in circulation.[7]

SULT1A3 is shown to play a role in the metabolism of various endogenous ligands—such as dopamine—however, it also is involved in the metabolism of exogenous ligands, such as resveratrol and salbutamol. Resveratrol, a compound found in red grape skin, red wine, and peanuts is a known anticancer agent.[11] It has been found to be metabolized through reactions catalyzed by sulfotransferases.[12] Resveratrol is also thought to reduce incidence of colon and breast cancer, as well as cardiovascular disease through its inhibition of cyclooxygenases.[13] This anticancer molecule is able to obstruct the activation of CRP1A1, which is a carcinogen-preventing agent, and can therefore stop cancer at the initial stage.[13] Resveratrol is sulfated to resveratrol-3-*O*-sulfate through a reaction mostly catalyzed by SULT1A1, but to a lesser degree also by SULT1A2, 1A3, and 1E1.[12] In a study by Miksits, *et al.* that investigated the involvement of resveratrol in preventing breast cancer, SULT1A1 and SULT1A3 were found to be expressed in the cytosol of breast tissue.[12] It was found that sulfation of resveratrol had a much higher incidence in samplings of cancerous breast tissue in comparison with the non-malignant tissue, indicating that there could be a correlation between sulfation of resveratrol and tissue expression of SULTs.[12]

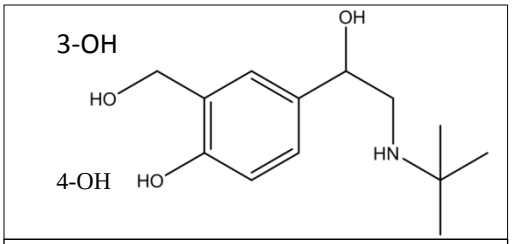

Figure 4. Structure of salbutamol with hydroxyl labeled.

Knowledge of the specificity of SULT1A3 is especially pertinent to the pharmaceutical understanding of the medication salbutamol, which is used to relieve symptoms of breathlessness associated with asthma and with chronic obstructive pulmonary disease.[14] SULT1A3 is regulated by glucocorticoids and exclusively metabolizes salbutamol, which makes it a target for additional studies because of its clinical significance.[8] Salbutamol is structurally similar to dopamine and has a benzylic and phenolic alcohol (Figure 4), which allows it to have similar interactions within the enzymatic active site.[14] In a study by Jacobson, *et al.*, the role of SULT1A3 in the metabolism of salbutamol is investigated.[14] Because this enzyme is so important to the metabolism of small phenolic structures similar to dopamine, variation in the specificity of the enzyme could affect the rate of the excretion of xenobiotics from the body.[14] Salbutamol is excreted from the body in urine in both its unchanged form and in the metabolite form.[14] For the metabolism of drugs, hepatic and intestinal SULT1A3 enzymes are of specific interest.

Understanding the process of sulfation of salbutamol is important in the both the food and pharmacological industries.[15] Salbutamol acts as a β-adrenergic agonist when added to feed for livestock.[15] Salbutamol is one of several feed additives used with the purpose of enhancing the leanness of the meat[15]. In a study by Ko, *et al.*, SULT1A3 was found to be the most prominent sulfotransferase in the metabolism of salbutamol with an activity of about 2.01 mmol/min/mg when exposed to 10μM of salbutamol.[15] In this study, the kinetic parameters of the sulfation of salbutamol were also investigated and could give

insight into the specificity of the enzyme.[15] The highest levels of sulfation of salbutamol was determined to be in the small intestine.[15] Salbutamol was found to inhibit the sulfation of dopamine in a concentration-dependent manner.[15] However, affinity of SULT1A3 for dopamine is higher than its affinity for salbutamol[15]. Therefore, it would require a high concentration of salbutamol to obstruct the homeostasis of dopamine or other endogenous ligands.[15] Salbutamol only has one phenolic hydroxyl group and thus the major product of sulfation of salbutamol has been found to be salbutamol-4-*O*-sulfate.[15]

Dajani, *et al.* studied the selectivity of the SULT1A3 active site though site-directed mutagenesis of Glu146.[2] The study concluded that the favorable interaction between the amine group of dopamine and Glu146 within the active site is the major factor for the specificity of dopamine and similar phenolic structures for SULT1A3.[2] Similarly, in a study by Brix, *et al.*, the authors used site-directed mutagenesis to study active sites of SULT1A3 and SULT1A1 by mutating Glu146Ala (E146A) and Ala146Glu (A146E), respectively; these mutations served the purpose of essentially making each active site resemble the other through these mutations.[16] Through this study, it was concluded that SULT1A3 demonstrates a preference for substrates containing an amine group as a substituent off of the aromatic ring.[16] Mutation of Glu146 to Ala in in SULT1A3 resulted in a K_m value for dopamine increased 8-fold, indicating that the enzyme no longer demonstrated a strong preference for dopamine.[16] Thus, the specificity constant was decreased by 64-fold, clearly showing a reduction in preference. After the A146E mutation, SULT1A1 continued to exhibit a high K_m value for dopamine and other ligands containing an amino tail.[16] The study by Brix, *et al.,* thus concluded that there is a direct

interaction between Glu146 in SULT1A3 and the substituent amine group on dopamine and similar molecules.[16]

1.2 Computational Methods

M062X is a DFT method, Density Functional Theory, which was developed Zhao and Truhlar, has been shown to accurately capture more electron correlation than previous methods and describes base pair stacking and hydrogen bonding correctly.[14] Second-order Møller-Plesset perturbation theory (MP2) is a method that takes noncovalent interactions, including some dispersion interactions, into account for the calculation of interactions energies.[11] As the active site of SULT1A3 contains amino acid residues that can participate in hydrogen bonds and π interactions with ligands these two computational methods were chosen.[17] The DFT method, M062X, is known to provide accurate energy calculations for a variety of non-covalent interactions, like those in SULT1A3.[10] The MP2 method, although shown to overestimate attractive energies, has been shown to correlate with interaction energy calculations in Coupled Cluster when used with a basis set larger than 6-31G*.[18]

In several sections of this project, optimizations were performed with implicit solvation with default settings for water using the Polarizable Continuum Model (PCM) of Tomasi, *et al.*[19] This calculation allows for improved charge distribution and dipole moments on the ligands and in the active site amino acids[20], which in turn leads to a better description of the intermolecular forces that depend on charge and charge distribution.[21] A study by Riley, *et al.* compared PCM calculations of hydrogen bond energies using both DFT (using the TPSS functional) and complete basis set MP2 +

CCSD(T) corrections.[21] They show good agreement between the two implicit solvation methods for O-based hydrogen bonds, and slightly worse agreement for N-based hydrogen bonds. The current work (see results below) shows much better agreement between M062X and MP2, both using the PCM solvation method, for both O-based and N-based hydrogen bonds.

2. Computational Details

The SULT1A3 active site was isolated from the crystal structure with a dopamine bound (PDB ID: 2A3R).[4] The active site was selected by proximity to the bound dopamine ligand and consists of Lys106, His108, His149, Glu146, Asp86, Ala148, Phe24, Phe81, Phe142, and Pro47. All the amino acid residues within the active site have an atom that is within 3.5 angstroms of an atom of the bound dopamine. Within the active site, the amino acid residues and the ligand were adjusted so that they were at the correct protonation state determined by biological pH. Each ligand was placed within the active site in two orientations: the first to favor deprotonation by His108 at the 3-position, and the second to favor deprotonation at the 4-position.

2.1 Model Chemistries

Dopamine, nine dopaminergic molecules with systematically varied substituents, two molecules lacking a positively charged tail, and resveratrol were used to investigate the accuracy of three computational models (Figure 5). Dopamine was selected for study because it is an endogenous ligand, selectively sulfated in SULT1A3.[3] The dopaminergic ligands have various electron-withdrawing or electron-donating properties with substituent groups substituted in the 6-position of the benzene ring. Resveratrol was investigated due to its preference for the SULT1A1 enzyme and thus predicted lower affinity for SULT1A3.

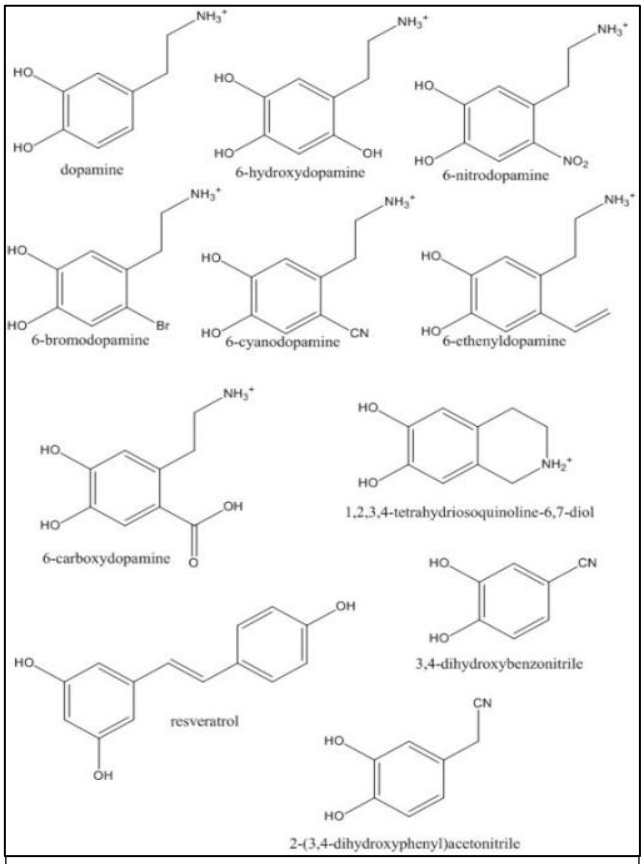

Figure 5. Ligands selected for study.

Optimizations of ligands within the active site were performed using M062X/6-31g. The ligand as well as the amino acid residue protons were allowed to optimize. Once the optimal structure was attained, the counterpoise-corrected interaction energies for each ligand-amino acid pair were calculated using the two methods—MP2 and M062x—both performed using a basis set of 6-311+g*. Total interaction energies were calculated by a summation of all ligand-amino-acid-residue interaction energies. This model chemistry is referred to as the vacuum-rigid (VR) model.

The solvated-rigid (SR) model includes the same optimization parameters as the VR model with the addition of implicit solvation by water using the Polarizable Continuum Model and the default setting for water.[19] Interaction energies were calculated in the same manner as in the VR model.

The solvated-relaxed (SX) model includes the same optimization parameters as the SR model with the addition of the optimization of the active site residue R-groups. During optimization, these groups were allowed to relax and move to the most energetically favorable position.

All calculations were performed using Gaussian09.[22]

2.2 Effective pKa

Calculations to find an effective pK_a were performed using parameters modeled by Zhang, *et al.*[23] The ligand, in both a protonated and deprotonated form, and an ammonium ion were optimized using the basis set OLYP/3-21g. The energies were then calculated from the optimized structures using a basis set of OLYP/6-311+g**. Optimizations were performed in gas phase and solvent phase with the polarizable continuum model with the default settings for water.[19]

2.3 Point Mutations

In this portion of the study, we investigated the effects of computational site-directed mutagenesis on the binding of dopamine, two dopaminergic analogues, and resveratrol to the SULT1A3 active site. The two analogues of dopamine, 6-carboxydopamine and 6-ethenyldopamine, were selected due to their interesting interactions within the SULT1A3 active site in previous work(Figure 6); these interactions are due to their electron

withdrawing and donating substituents at the 6-position.[22] In our previous research, 6-carboxydopamine and 6-ethenyldopamine were found to have the strongest interaction energy and the weakest interaction energy, respectively, out of the nine ligands studied.[25] Resveratrol was again selected due to its known affinity for the SULT1A1 active site and its importance as an antioxidant and anti-cancer compound.[11]

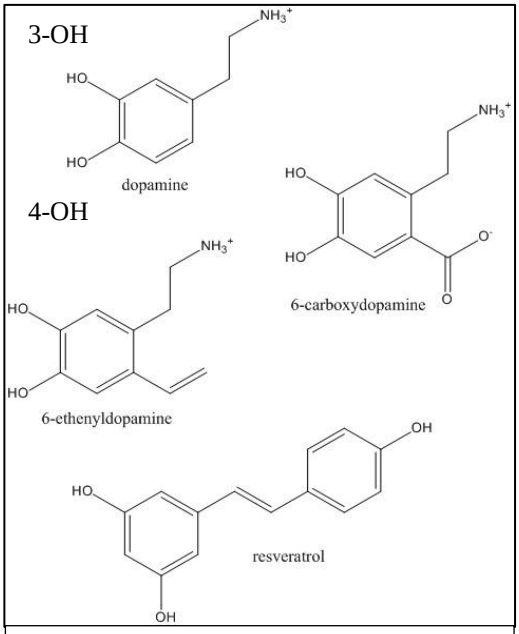

Figure 6. Ligands investigated in point mutations study.

The interaction of each ligand with the active site was calculated in eight ways. Each ligand was analyzed in the wild type (wt) active site (these data are reported in the the Appendix: (A1-A3[25])), as well as in the two mutant active sites, D86A and E146A and the doubly mutated active site D86A + E146A. For each ligand in each of the four active sites, the ligand was positioned so that either the 3- or 4-hydroxy groups (see Figure 6) would be deprotonated by His108, leading to two different products of sulfation.[14] For the first mutant, D86A, the side chain on the D86 residue was changed to an alanine side chain. Then the ligands were optimized in the active site using M062X/6-31G allowing for all amino acid residue side chains to relax and including implicit solvation with water. Each ligand/active site complex was optimized twice, favoring deprotonation of the hydroxyl group at the 3-position or at the 4-position of the ligand. After optimization, all ligand/amino-acid pairs were isolated (capping amino acid residues with –OH or –H to maintain the charge and polarity found in the protein) and counterpoise-corrected

interaction energies for all ligand-residue pairs were calculated with two methods, MP2 and M062X, both with a basis set of 6-311+G*.[26] The total interaction energy for each ligand was calculated as a sum of the pairwise interaction energies of the ligand with each amino acid. For the second mutant (E146A), the E146 residue was changed to alanine and the above calculations were repeated. Finally, both mutations were made simultaneously (D86A and E146A) and the calculations were repeated a third time.

2.4 Salbutamol

Salbutamol, in its four different conformations, was investigated in this study. The active site that was used for SULT1A3 was obtained from a crystal structure with bound dopamine and contains ten amino acid residues.[4] The first orientation of salbutamol favors sulfation at the 4-position; the second favors sulfation at the 4-position, but in a flipped orientation of the ligand. Similarly, in the third and fourth orientations, salbutamol is oriented to allow for deprotonation at the 3-position.

Salbutamol within the active site was optimized using M062X with a basis set of 6-31G using the SX model described above. Salbutamol was optimized in the four previously defined positions and then interaction energies were calculated as described above. Two methods were used for the calculation of the counterpoise-corrected interaction energy, MP2 and M062X, both with a basis set of 6-311+G*.[19] The total interaction energy was calculated by a summation of the individual ligand/active site calculations.

Results and Discussion

3.1 Model Chemistries

3.1.1 Optimizations and Structures

The major findings in the work described in this section have been previously published.[25]

Figure 7 shows the optimized structure in the VR model, with the hydroxyl group in the 3-position of the ligands positioned so that it will be favored for sulfation. Lys106 and His108, which were previously noted to be important to the catalytic part of sulfation are seen in the left side of each image; the lysine residue stabilizes the hydroxyl group as the histidine residue abstracts the proton from the ligand. In the cases of dopamine, hydroxydopamine, 'cyclic' dopamine, bromodopamine, cyanodopamine, ethenyldopamine, carboxydopamine, resveratrol, 3,4-dihydroxybenzonitrile, and 2-(3,4-dihydroxyphenyl)acetonitrile, the proton was not abstracted from the 3-position hydroxyl group of the ligand after optimization using the VR model. The only case where the proton is abstracted by His108 after optimization is nitrodopamine. In this conformation, the amino tail remains positively charged after optimization in dopamine, 'cyclic' dopamine, and carboxydopamine. The amino acid group becomes neutral in hydroxydopamine, nitrodopamine, bromodopamine, cyanodopamine, and ethenyldopamine. The neutral charge on the amino tail of the dopaminergic ligands occurs due to the abstraction of a proton by the Asp86 residue in the active site. This mechanism for proton abstraction of the tail is common to all of the current calculations.

Figure 8 shows the optimized structure in the VR model, with the hydroxyl group in the 4-position of the dopaminergic ligands or the 5-position of resveratrol positioned so that it will be favored for sulfation. In the cases of dopamine, hydroxydopamine, 'cyclic' dopamine, nitrodopamine, bromodopamine, ethenyldopamine, carboxydopamine, resveratrol, dihydroxybenzonitrile, and (dihydroxyphenyl)acetonitrile, the proton was not

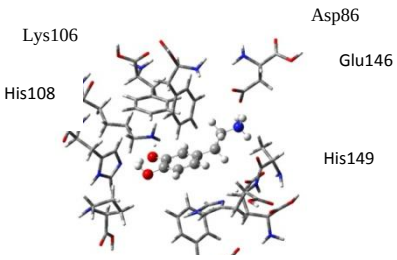

dopamine
(1.53, 1.06)(1.08, 1.53)

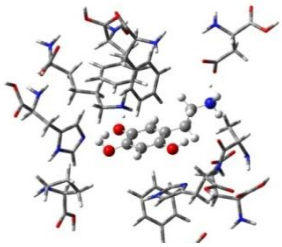

6-hydroxydopamine
(1.53, 1.05)(1.09, 1.52)

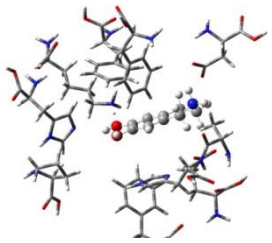

1,2,3,4-tetrahydroiso quinoline-6,7-diol
(2.39, 0.99)(1.06, 1.60)

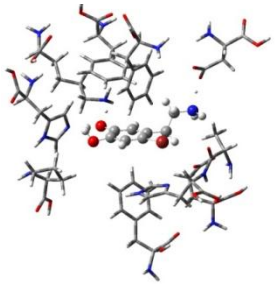

6-nitrodopamine
(1.12, 1.42)(1.12, 1.45)

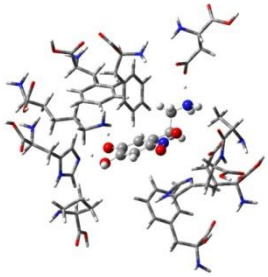

6-bromodopamine
(1.41, 1.09)(1.09, 1.52)

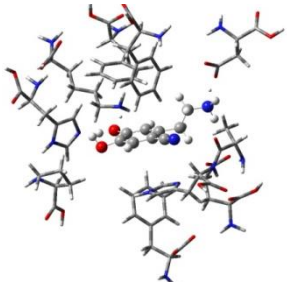

6-cyanodopamine
(1.43, 1.09)(1.08, 1.55)

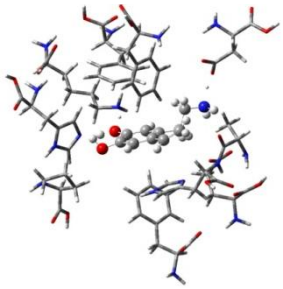

6-ethenyldopamine
(1.48, 1.07)(1.08, 1.59)

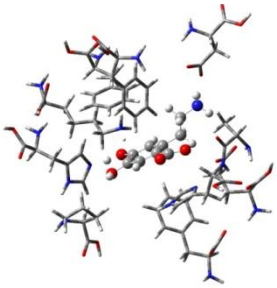

6-carboxydopamine
(1.31, 1.15)(1.14, 1.39)

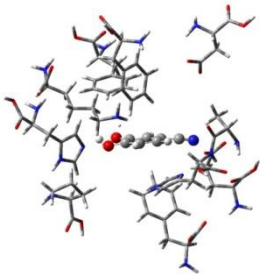

3,4-dihydroxybenzonitrile
(1.53, 1.05)(1.08, 1.53)

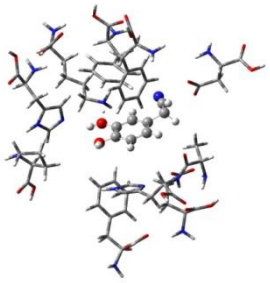

2-(3,4-dihydroxyphenyl)acetonitrile
(2.21, 0.985)(1.07, 1.59)

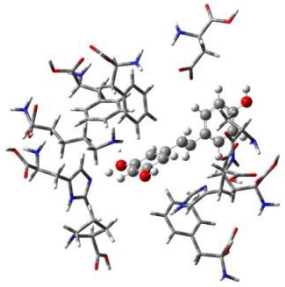

resveratrol
(1.09, 1.51)(1.51, 1.05)

Figure 7. *In vacuo* optimized structures (M062X/6-31G) of the nine ligands in the active site using rigid amino acid residues (VR model). Ligands are arranged to be deprotonated at the 3-position. The data in parentheses are the distances (Å) from (His108 to the proton, Ligand to the proton) (Lys106 to the proton, Ligand to the Proton).

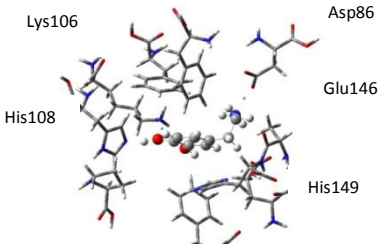

dopamine
(1.31, 1.15)(1.09, 1.45)

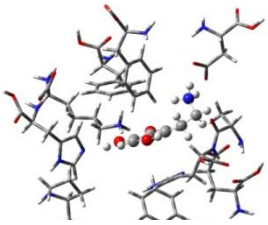

6-hydroxydopamine
(1.73, 1.02)(1.06, 1.58)

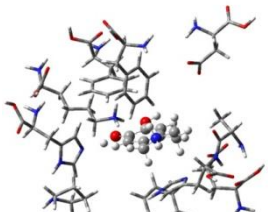

1,2,3,4-tetrahydroiso quinoline-6,7-diol
(1.66, 1.03)(1.06, 1.64)

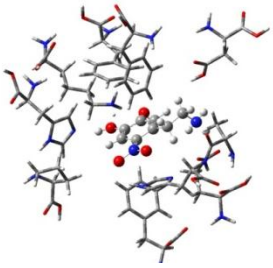

6-nitrodopamine
(1.79, 0.994)(1.11, 1.45)

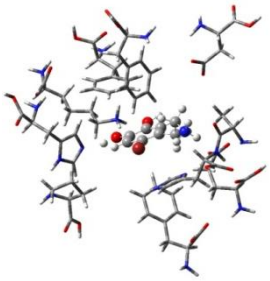

6-bromodopamine
(1.56, 1.04)(1.06, 1.60)

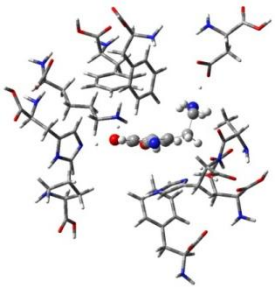

6-cyanodopamine
(1.14, 1.38)(1.12, 1.38)

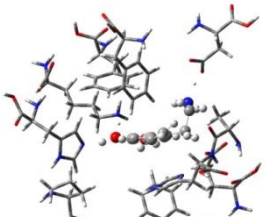

6-ethenyldopamine
(1.53, 1.06)(1.08, 1.53)

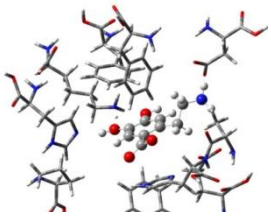

6-carboxydopamine
(1.88, 1.00)(1.07, 1.46)

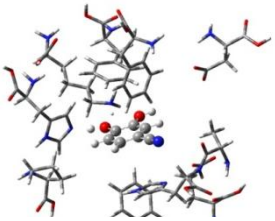

3,4-dihydroxybenzonitrile
(1.46, 1.07)(1.07, 1.55)

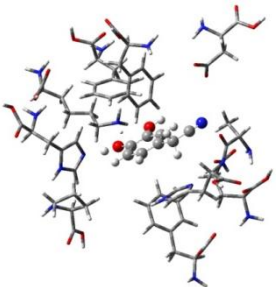

2-(3,4-dihydroxyphenyl)acetonitrile
(1.52, 1.05)(1.07, 1.54)

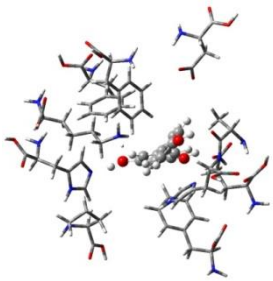

resveratrol
(1.57, 1.04)(1.09, 1.45)

Figure 8. *In vacuo* optimized structures (M062X/6-31G) of the nine ligands in the active site using rigid amino acid residues (VR model). Ligands are arranged to be deprotonated at the 4-position. The data in parentheses are the distances (Å) from (His108 to the proton, Ligand to the proton) (Lys106 to the proton, Ligand to the Proton).

abstracted from the hydroxyl group of the ligand after optimization using the VR model. The only case where the proton is abstracted by His108 in the optimized strucure is in the case of cyanodopamine. In this conformation, the amino tail remains positively charged after optimization in hydoxydopamine, 'cyclic' dopamine, nitrodopamine, bromodopamine, and carboxydopamine. The amino acid group becomes neutral in dopamine, cyanodopamine, and ethenyldopamine.

The optimized structure in the SR model, with the hydroxyl group in the 3-position of the ligands positioned so that it will be favored for sulfation is shown in Figure 9. In the cases of dopamine, hydroxydopamine, 'cyclic' dopamine, ethenyldopamine, resveratrol, dihydroxybenzonitrile, and (dihydroxyphenyl)acetonitrile, the proton was not abstracted from the hydroxyl group in the 3-position of the ligand after optimization using the SR model. The cases where the proton is abstracted by His108 are nitrodopamine, bromodopamine, cyanodopamine, and carboxydopamine. In this conformation, the amino tail remains positively charged after optimization in dopamine, hydroxydopamine, 'cyclic' dopamine, nitrodopamine, bromodopamine, cyanodopamine, and carboxydopamine. The amino acid group becomes neutral only in ethenyldopamine.

Figure 10 shows the optimized structure in the SR model, with the hydroxyl group in the 4-position of the dopaminergic ligands or the 5-position of resveratrol positioned so that it will be favored for sulfation. In the cases of hydroxydopamine, 'cyclic' dopamine, bromodopamine, carboxydopamine, and (dihydroxyphenyl)acetonitrile, the proton was not abstracted from the respective hydroxyl group of the ligand after optimization using the SR model. In the cases of dopamine, nitrodopamine, cyanodopamine, ethenyldopamine, dihydroxybenzonitrile, and resveratrol the proton was abstracted by

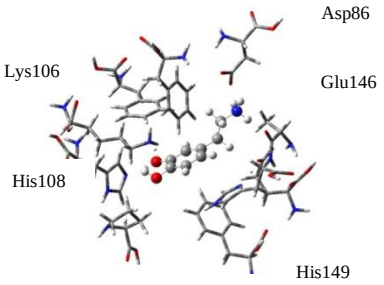

dopamine
(1.49, 1.07)(1.07, 1.58)

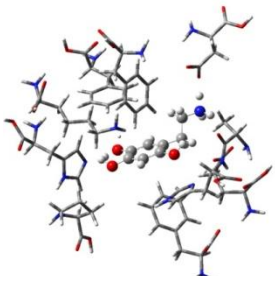

6-hydroxydopamine
(1.47, 1.07)(1.07, 1.58)

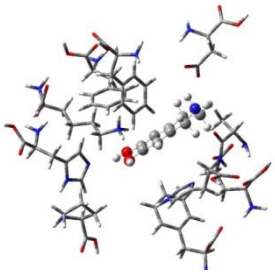

1,2,3,4-tetrahydroiso quinoline-6,7-diol
(2.10, 0.992)(1.06, 1.60)

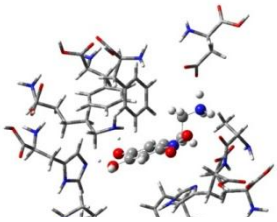

6-nitrodopamine
(1.07, 1.52)(1.09, 1.51)

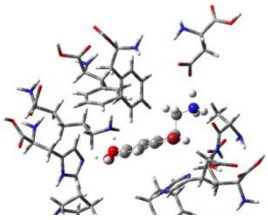

6-bromodopamine
(1.12, 1.41)(1.12, 1.43)

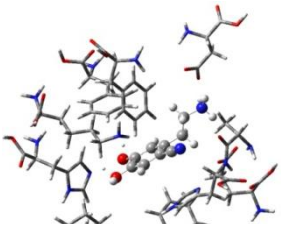

6-cyanodopamine
(1.07, 1.56)(1.12, 1.45)

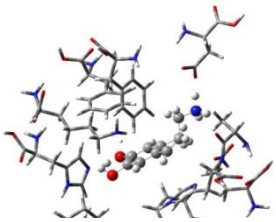

6-ethenyldopamine
(1.43, 1.09)(1.06, 1.65)

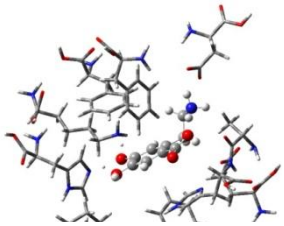

6-carboxydopamine
(1.11, 1.44)(1.14, 1.41)

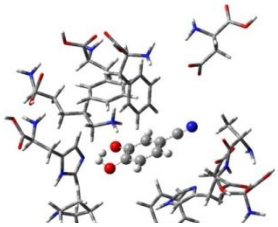

3,4-dihydroxybenzonitrile
(1.46, 1.08)(1.06, 1.66)

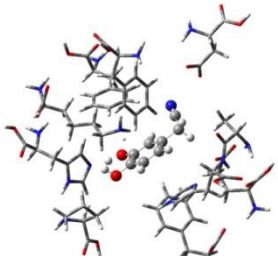

2-(3,4-dihydroxyphenyl)acetonitrile
(1.40, 1.10)(1.07, 1.62)

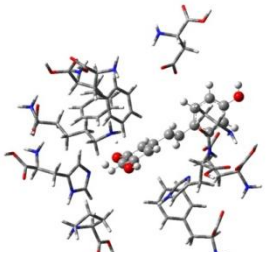

resveratrol
(1.42, 1.09)(1.07, 1.57)

Figure 9. . PCM (water) optimized structures (M062X/6-31G) of the nine ligands in the active site using rigid amino acid residues (SR model). Ligands are arranged to be deprotonated at the 3-position. The data in parentheses are the distances (Å) from (His108 to the proton, Ligand to the proton) (Lys106 to the proton, Ligand to the Proton).

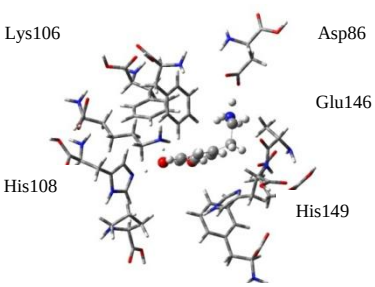

dopamine
(1.10, 1.46)(1.13, 1.37)

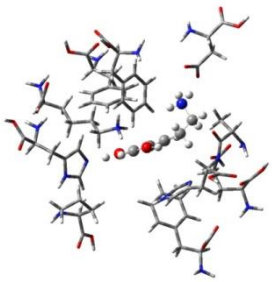

6-hydroxydopamine
(1.45, 1.09)(1.06, 1.60)

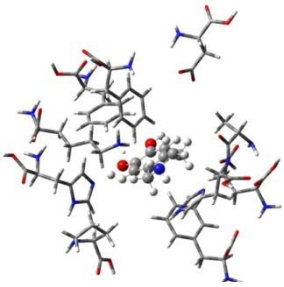

1,2,3,4-tetrahydroiso quinoline-6,7-diol
(1.44, 1.08)(1.06, 1.59)

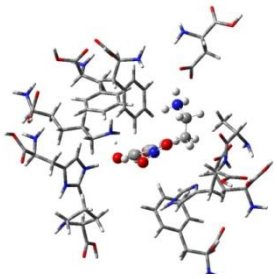

6-nitrodopamine
(1.06, 1.65)(1.10, 1.47)

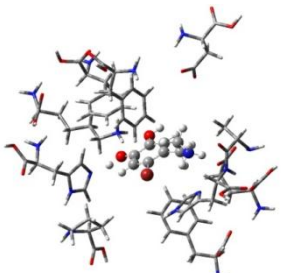

6-bromodopamine
(1.48, 1.07)(1.06, 1.62)

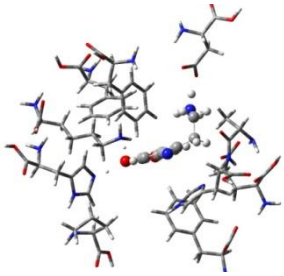

6-cyanodopamine
(1.07, 1.55)(1.12, 1.40)

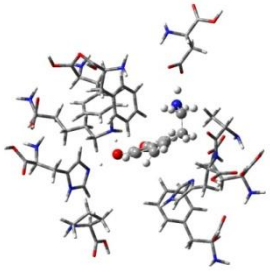

6-ethenyldopamine
(1.08, 1.51)(1.13, 1.38)

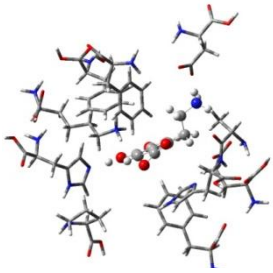

6-carboxydopamine
(1.53, 1.06)(1.06, 1.59)

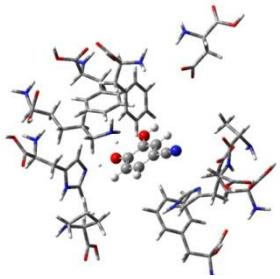

3,4-dihydroxybenzonitrile
(1.17, 1.32)(1.08, 1.55)

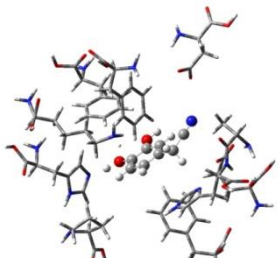

2-(3,4-dihydroxyphenyl)acetonitrile
(1.42, 1.09)(1.06, 1.60)

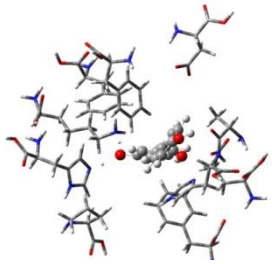

resveratrol
(1.07, 1.56)(1.18,

Figure 10. . PCM (water) optimized structures (M062X/6-31G) of the nine ligands in the active site using rigid amino acid residues (SR model). Ligands are arranged to be deprotonated at the 4-position. The data in parentheses are the distances (Å) from (His108 to the proton, Ligand to the proton) (Lys106 to the proton, Ligand to the Proton).

His108. In this conformation, the amino tail remains positively charged after optimization in all of the dopaminergic ligands.

Figure 11 shows the optimized structure in the SX model, with the hydroxyl group in the 3-position of the ligands positioned so that it will be favored for sulfation. In the cases of dopamine, hydroxydopamine, 'cyclic' dopamine, and ethenyldopamine, the proton was not abstracted from the hydroxyl group in the 3-position of the ligand after optimization using the SX model. The cases where the proton is abstracted by His108 are nitrodopamine, bromodopamine, cyanodopamine, carboxydopamine, dihydroxybenzonitrile, (dihydroxyphenyl)acetonitrile, and resveratrol. In this conformation, the amino tail remains positively charged after optimization in all of the dopaminergic ligands.

Figure 12 shows the optimized structure in the SX model, with the hydroxyl group in the 4-position of the dopaminergic ligands or the 5-position of resveratrol positioned so that it will be favored for sulfation. The proton was abstracted from the respective hydroxyl group of the ligand in all the cases after optimization using the SX model. In this conformation, the amino tail remains positively charged after optimization in dopamine, hydroxydopamine, 'cyclic' dopamine, nitrodopamine, ethenyldopamine, and carboxydopamine. The amino acid group becomes neutral in bromodopamine and cyanodopamine.

Most notable in the above struture optimization results is the formation of charges in the optimization process. In the VR model (the least realistic), only one ligand in each of the two conformations (3- or 4- deprotonation) is deprotonated, leaving a negatively charged oxygen atom. In the first implicit solvent model (SR), four ligands have a deprotonated,

negative oxygen atom in the 3- position and five ligands have a negative oxygen in the 4/5- position. Finally, in the solvated, relaxed model (SX), five ligands have negative, deprotonated oxygen atoms in the 3- position conformers, and all nine ligands are deprotonated in the 4/5- position. This shows that solvation and relaxation promote ion formation, change hydrogen bonds into ion/ion interactions and increase interaction energy.

We can similarly examine the NH_3^+ 'tails' of the ligands in all the optimizations. In the VR model, three and five ligands have charged tails in the 3- and 4/5- positions, respectively. In the SR model, seven and nine (all) ligands have charged tails in the 3- and 4/5- positions, respectively. Finally, in the SX model, nine and seven ligands have charged tails in the 3- and 4/5- positions, respectively. Again, this shows the more realistic models favoring ion formation and stronger intermolecular forces.

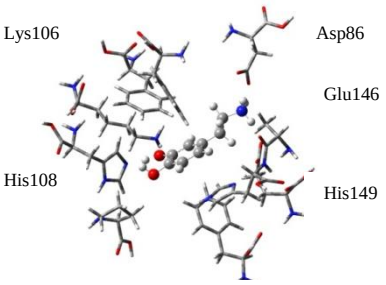

dopamine
(1.45, 1.09)(1.07, 1.60)

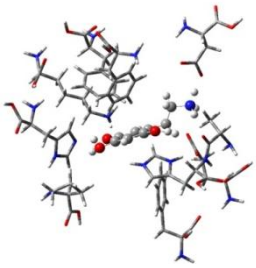

6-hydroxydopamine
(1.50, 1.06)(1.06, 1.62)

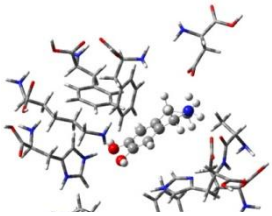

1,2,3,4-tetrahydroiso
quinoline-6,7-diol
(1.06, 1.62)(1.37, 1.38)

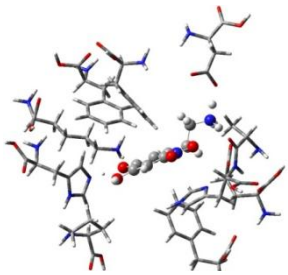

6-nitrodopamine
(1.07, 1.54)(1.09, 1.53)

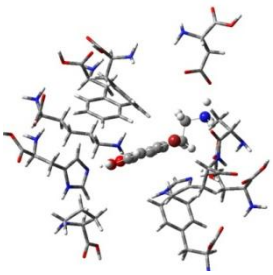

6-bromodopamine
(1.09, 1.49)(1.15, 1.38)

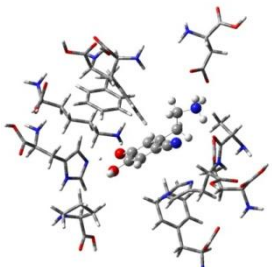

6-cyanodopamine
(1.07, 1.56)(1.12, 1.43)

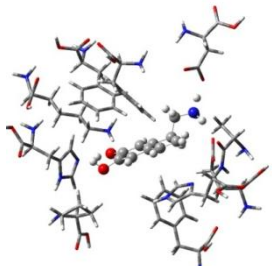

6-ethenyldopamine
(1.52, 1.06)(1.06, 1.64)

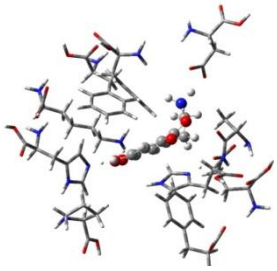

6-carboxydopamine
(1.07, 1.57)(1.20, 1.29)

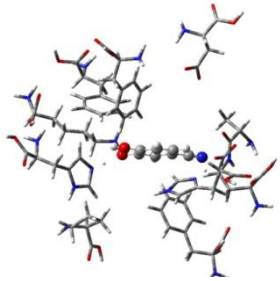

3,4-dihydroxybenzonitrile
(1.06, 1.57)(1.14, 1.39)

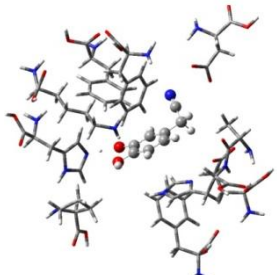

2-(3,4-dihydroxyphenyl)acetonitrile
(1.53, 1.05)

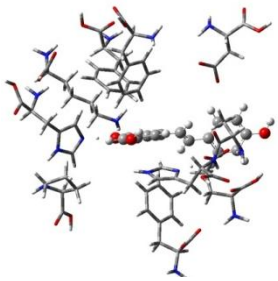

resveratrol
(1.15, 1.36)(1.13, 1.42)

Figure 11. PCM (water) optimized structures (M062X/6-31G) of the nine ligands in the active site using relaxed amino acid residues (SX model). Ligands are arranged to be deprotonated at the 4-position. The data in parentheses are the distances (Å) from (His108 to the proton, Ligand to the proton) (Lys106 to the proton, Ligand to the Proton).

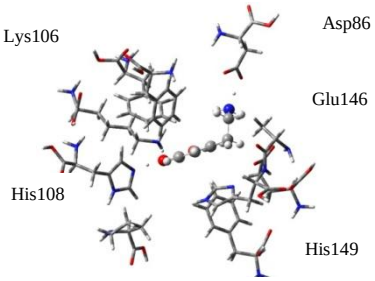

dopamine
(1.16, 1.33)(1.11, 1.45)

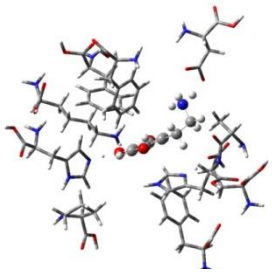

6-hydroxydopamine
(1.14, 1.36)(1.11, 1.46)

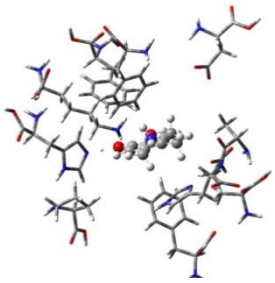

1,2,3,4-tetrahydroiso quinoline-6,7-diol
(1.17, 1.32)(1.10, 1.49)

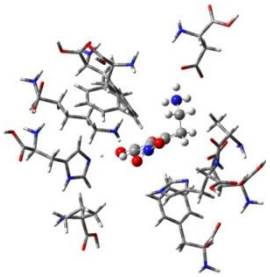

6-nitrodopamine
(1.07, 1.58)(1.10, 1.47)

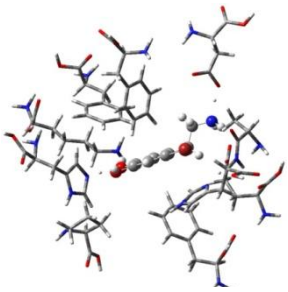

6-bromodopamine
(1.06, 1.56)(140, 1.12)

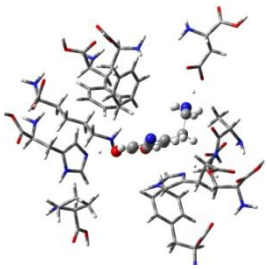

6-cyanodopamine
(1.11, 1.41)(1.10, 1.46)

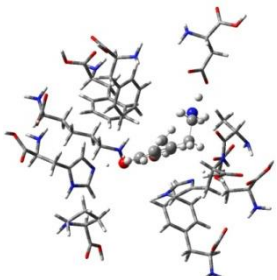

6-ethenyldopamine
(1.15, 1.35)(1.11, 1.45)

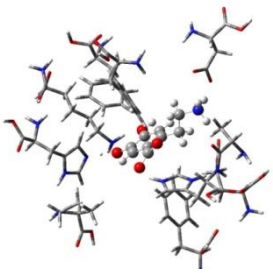

6-carboxydopamine
(1.18, 1.30)(1.10, 1.48)

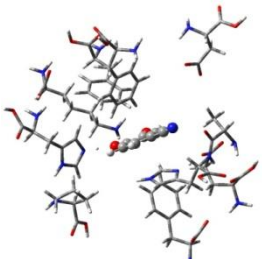

3,4-dihydroxybenzonitrile
(1.11, 1.44)(1.09, 1.51)

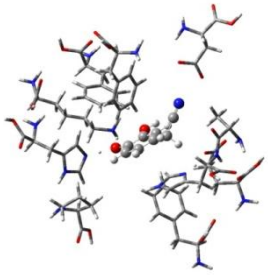

2-(3,4-dihydroxyphenyl)acetonitrile
(1.17, 1.32)(1.10, 1.47)

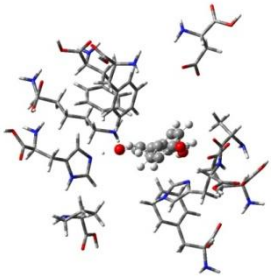

resveratrol
(1.10, 1.45)(1.18, 1.31)

Figure 12. PCM (water) optimized structures (M062X/6-31G) of the nine ligands in the active site using relaxed amino acid residues (SX model). Ligands are arranged to be deprotonated at the 4-position. The data in parentheses are the distances (Å) from (His108 to the proton, Ligand to the proton) (Lys106 to the proton, Ligand to the Proton) in nm.

3.1.2 Interaction Energies

The results for the VR, SR, and SX models, respectively are shown in Tables 1, 2, and 3. Tables A1, A2 and A3 (Appendix) show a summary of each of the three models useful for comparisons. In these summary tables, it is shown for each ligand if deprotonation at the 3- or 4-position is favored (by a lower interaction energy between the ligand in each particular conformation and the active site residues), the MP2 total interaction energy for the favored conformer, and each molecule's rank order in terms of interaction energy.

Table 1: Summary for the Vacuum-Rigid model. The second column shows if deprotonation is favored at the 3 or 4 position. Counterpoise-corrected MP2 interaction energies are in kcal/mol. Rank indicates strongest to weakest interaction.[25]

Molecule	3 or 4 favored?	Interaction Energy	Rank
Dopamine	3	-118	5
6-hydroxydopamine	4	-125	4
"cyclic"-dopamine	3	-95	6
6-nitrodopamine	3	-254	2
6-bromodopamine	4	-77	7
6-cyanodopamine	4	-264	1
6-ethenyldopamine	even	-62	8
6-carboxydopamine	4	-156	3
3,4-dihydroxybenzonitrile	4	-36	11
2-(3,4-dihydroxyphenyl)acetonitrile	3	-42	10
resveratrol	even	-48	9

The crystal structure used here was obtained with dopamine bound, so it should favor dopamine and dopamine derivatives. For the VR model, the MP2 and M062X methods agree very well, with an average difference between total interaction energies of 14.0 kcal/mol (Table A1). The M062X method predicts lower interaction energies (more

tightly bound) in all cases except the 3-position conformer of 6-carboxydopamine. In most cases, the differences between MP2 and M062X for the individual ligand-amino-acids interaction energies are smaller than those for the total. His108 and Lys106, the two residues involved in the deprotonation of the hydroxyl group, generally have the largest interaction energies (Table A1). These can range from roughly -6 kcal/mol for the cases where the interaction is a hydrogen bond, to roughly -100 kcal/mol in the cases where the proton is transferred and an ionic interaction between the residues and the ligand result. The 'tails' of the dopaminergic ligands all have a protonated $–NH_3^+$ group ($–NH_2^+$ for the 'cyclic' dopamine), which can form favorable interactions with the negatively charged Asp86 and Glu146 residues in the active site. These interactions are typically on the order of roughly -10-50 kcal/mol, again, depending on whether they are hydrogen bonds or partial ionic interactions. The ligands that lack the protonated NH_3^+ group show interaction energies that indicate they are the least strongly bound.

Overall, the VR model is split between deprotonation on the 3- and 4-positions (Table 1). Dopamine, 'cyclic' dopamine, nitrodopamine, and 3,4-dihydroxybenzonitrile favor the 3-position, while the others either favor the 4-position or are evenly-split (*i.e.* the energy difference between sulfation at the 3- and 4-hydroxyl group is less than 10 kcal/mol). The average interaction energy for the nine ligands is -116 kcal/mol, with an average deviation of 61 kcal/mol. 6-Cyanodopamine is the most strongly bound ligand, while 3,4-dihydroxybenzonitrile is the least strongly bound.

For the SR model, again, the MP2 and M062X methods agree very well, with an average difference between total interaction energies of 8.4 kcal/mol (Table A2). The M062X method predicts lower interaction energies (more tightly bound) in all cases. His108 and

Lys106 generally have the largest interaction energies, which range from roughly -7 kcal/mol to roughly -113 kcal/mol depending on the type of interaction between the residues and the ligand (Table A2). In a few cases, the interaction with Lys106 is strongly repulsive (roughly +30 kcal/mol). This results when the ligand has an overall positive charge, which repels the positively-charged lysine. The positive charge on the ligand is due to an $-NH_3^+$ on the tail of the molecule and no deprotonation on the phenolic hydroxyl groups. The positive tail still has favorable interactions with negatively-charged Asp86 and Glu146.

Table 2: Summary for the Solvated-Rigid model. The second column shows if deprotonation is favored at the 3 or 4 position. Counterpoise-corrected MP2 interaction energies are in kcal/mol. Rank indicates strongest to weakest interaction.[25]

Molecule	3 or 4 favored ?	Interaction Energy	Rank
dopamine	4	-202	5
6-hydroxydopamine	even	-121	9
"cyclic"-dopamine	3	-92	10
6-nitrodopamine	even	-172	8
6-bromodopamine	3	-210	3
6-cyanodopamine	even	-192	7
6-ethenyldopamine	4	-199	6
6-carboxydopamine	3	-258	1
3,4-dihydroxybenzonitrile	4	-203	4
2-(3,4-dihydroxyphenyl)acetonitrile	even	-35	11
Resveratrol	4	-214	2

The SR model is an improvement over the VR model in terms of the strengths of the interaction energies. It is again split between deprotonation on the 3- and 4-positions (Table 2). In this model, ‘cyclic’ dopamine, 6-bromodopamine and 6-carboxydopamine

favor the 3- position, while the others either favor the 4-position or are evenly-split. The average interaction energy for the nine ligands is -173 kcal/mol, with an average deviation of 49 kcal/mol. The presence of the implicit solvent stabilizes charges and allows more of the hydrogen bonds formed in the VR model to change into ionic bonds (via proton transfers). This makes the interactions more attractive than in the VR model on average by 57 kcal/mol. Further, this more 'realistic' model has decreased the average deviation of the interactions, suggesting that the rather large differences in the VR model are artifacts. This model suggests that all nine ligands bind with much more similar interaction strengths. 6-Carboxydopamine is the most strongly bound ligand, while 2-(3,4-dihydroxyphenyl)acetonitrile is the least strongly bound. 'Cyclic' dopamine was the least strongly bound of the dopaminergic analogues. In comparison with the VR model, ligands with electron withdrawing ethenyl groups moved down in interaction strength rank-order, and ligands with electron-donating groups moved upwards.

For the SX model, again, the MP2 and M062X methods agree very well, though the average difference between total interaction energies is lower than the two previous models at 5.1 kcal/mol (Table A3). The M062X method predicts lower interaction energies (more tightly bound) in all cases. His108 and Lys106 generally have the largest interaction energies, which range from roughly -15 kcal/mol to roughly -129 kcal/mol depending on the type of interaction between the residues and the ligand (Table A3). As with the SR model, there are a few cases where the interaction with Lys106 is strongly repulsive (roughly +30 kcal/mol). Again, this results when the ligand has an overall positive charge, which repels the positively-charged lysine. The positive tail still generally has favorable interactions with negatively-charged Asp86 and Glu146.

Table 3: Summary for the Solvated-Relaxed model. The second column shows if deprotonation is favored at the 3 or 4 position. Counterpoise-corrected MP2 interaction energies are in kcal/mol. Rank indicates strongest to weakest interaction. [25]

Molecule	3 or 4 favored ?	Interaction Energy	Rank
dopamine	4	-248	5
6-hydroxydopamine	4	-261	3
"cyclic"-dopamine	even	-178	11
6-nitrodopamine	3	-229	8
6-bromodopamine	3	-260	4
6-cyanodopamine	4	-280	2
6-ethenyldopamine	4	-248	6
6-carboxydopamine	4	-405	1
3,4-dihydroxybenzonitrile	4	-195	10
2-(3,4-dihydroxyphenyl)acetonitrile	even	-227	9
Resveratrol	even	-241	7

The SX model shows improvement when compared to the VR and SR models in two regards. First, interaction energies are stronger and more consistent across all molecules, and second, the large changes in ordering that occurred between VR and SR have mostly leveled-off. This model is again split between deprotonation on the 3- and 4-positions (Table 3). In this model, 6-bromodopamine and 6-nitrodopamine favor the 3-position, while the others either favor the 4-position or are evenly-split. The average interaction energy for the nine ligands is -252 kcal/mol, with an average deviation of 36 kcal/mol. The presence of the implicit solvent stabilizes charges and the relaxation of the side chains allows for better accomodation of the ligands in the active site. These factors make the interactions more attractive than those in the SR model on average by 80 kcal/mol. Further, this most ‘realistic’ of the models studied here has a lower average deviation

among the interactions, supporting the premise that the rather large differences in interactions in the VR model are artifacts. 6-Carboxydopamine, as in the SR model, is the most strongly bound ligand, while ‘cyclic’ dopamine, as in the SR model, is the least strongly bound. The fact that there was less change in the 3-/4- preference and in the rank ordering of the ligands between the SR model and the SX model suggests that the model chemistry is converging. The main change in SX when compared with SR is that 6-cyanodopamine and 6-hydroxydopamine moved higher in interaction rank order. Also, 2-(3,4-dihydroxylphenyl)acetonitrile is ranked lower in Table A3.

One of the more notable results from this work is that 6-nitrodopamine, despite having the most electron-withdrawing substituent of all of the ligands studied here, has the second lowest interaction energy of the dopaminergic ligands in the more realistic SX model (Table 3). Also, the two ligands lacking the positively-charged amino tail were ranked lower in the SX model (Table 3). In the VR model, it has an interaction energy of -254 kcal/mol, very close to the -264 kcal/mol of 6-cyanodopamine (Table 1). This is expected, as the nitro and cyano groups generally have very similar behavior as substituents on rings. However, once implicit solvent is introduced, the interaction energy for the nitrodopamine decreases relative to the cyanodopamine. This may be explained by the fact that, in our ongoing experimental study, 6-nitrodopamine is more hydrophobic than the other ligands and is the only ligand studied so far that had to be dissolved in DMSO. If this is the case, the binding affinity would be further reduced, as less strongly-held water molecules will be displaced and generate entropic contributions for the free energy.

3.2 Effective pKa

The pK_a of both hydroxyl groups on each ligand was calculated in order to estimate the 'ease of deprotonation' at each site (Table 4). The pK_a was calculated for the isolated ligands with an NH_4^+ stabilizing the oxygen atom targeted for deprotonation (Figure 13) .This was done to simulate the stabilization by Lys106 present in the active site. Six of the nine ligands show that the 4-position is more easily deprotonated (correlating with the interaction energy results that show that the majority of the ligands are more stable in the 4-deprotonation and subseqent sulfation conformation). The lowest pK_a's belong to nitrodopamine and cyanodopamine, again showing that these two substituents behave similarly as far as influencing the electronic strucure of the ligand. The highest pK_a's belong to the two most hydrophobic ligands, resveratrol and 6-ethenyldopamine. These are also two of the least strongly interacting ligands in the SX model.

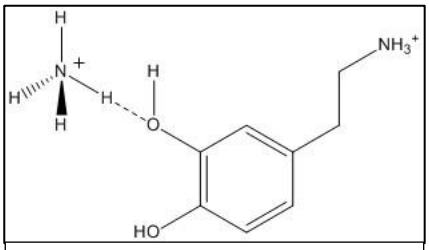

Figure 13. NH_4^+ molecule stabilizing dopamine.

Table 4: Calculated pK_a for both hydroxyl groups on each ligand.
pK_a calculated using the parameters of Zhang *et al.*[23]

	Effective pKa
Dopamine 3-OH	3.20
Dopamine 4-OH	2.78
6-hydroxydopamine 3-OH	3.60
6-hydroxydopamine 4-OH	3.02
1,2,3,4-tetrahydroisoquinoline-6,7-diol 3-OH	3.40
1,2,3,4-tetrahydroisoquinoline-6,7-diol 4-OH	2.62
6-nitrodopamine 3-OH	2.14
6-nitrodopamine 4-OH	2.71
6-bromodopamine 3-OH	2.80
6-bromodopamine 4-OH	2.23
6-cyanodopamine 3-OH	2.64
6-cyanodopamine 4-OH	1.80
6-ethenyldopamine 3-OH	4.67
6-ethenyldopamine 4-OH	4.55
6-carboxydopamine 3-OH	3.44
6-carboxydopamine 4-OH	3.55
3,4-dihydroxybenzonitrile 3-OH	2.90
3,4-dihydroxybenzonitrile 4-OH	2.87
2-(3,4-dihydroxyphenyl)acetonitrile 3-OH	3.58
2-(3,4-dihydroxyphenyl)acetonitrile 4-OH	3.57
Resveratrol 3-OH	4.15
Resveratrol 5-OH	4.16

3.3 Point Mutations

In the point mutations portion of the calculations, the results generated by the MP2 and M062X methods correlated well with each other, with an average difference of 12.4 kcal/mol between interaction energies calculated with each method. Overall, the M062X method produced calculations that suggest a slightly more attractive force between the ligand and the active site. Due to the overall agreement between the methods, in most of the discussion below only the MP2 values will be referenced. Table 5 shows the results for the wt and three mutant active sites interacting with each ligand. While interaction energies for all ligand/amino acid pairs were calculated (see supplementary data), the six amino acid residues that are presented in Table A4 were selected due to their significant individual interaction energies with the ligand. The strongest total interaction energy across all ligands is from 6-carboxydopamine (-381 kcal/mol) with the D86A mutation, favoring the 4-position for deprotonation. The weakest calculated interaction energy was dopamine with double mutant, in the orientation favoring the 3-position for deprotonation (56.4 kcal/mol, repulsive).

Table 5. Counterpoise-corrected MP2 interaction energies for ligands optimized with relaxed amino acid residues and implicit solvation. wt Interaction Energies taken for comparison from previous work.[25] Energies in kcal/mol.

Ligand	Total Interaction Energy			
	wt	D86A	E146A	D86A + E146A
Dopamine 3-OH	-178	-63.8	-229	56.4
Dopamine 4-OH	-246	-125	-229	-150
6-Carboxydopamine 3-OH	-265	-266	-339	-335
6-Carboxydopamine 4-OH	-397	-381	-377	-358
6-Ethenyldopamine 3-OH	-166	-56.4	-56.0	41.7
6-Ethenyldopamine 4-OH	-248	-170	-344	-151
Resveratrol 3-OH	-239	-274	-282	-315
Resveratrol 5-OH	-230	-271	-270	-310

The optimized structures of ligands bound in the SULT1A3 active site with the D86A mutation were calculated (Figure 14); dopamine with the 3-OH position favored for deprotonation is shown with the major amino acid residues labeled. In the case of all the orientations of the dopaminergic ligands, the amino tail retained its third proton and is thus locally positively-charged. This local positive charge in this position of the active site allows for a favorable interaction between His149 and each ligand. In the case of dopamine and 6-ethenyldopamine with the 3-OH position favored for deprotonation, the ligand retained the 3-hydroxyl proton (*i.e.*, it was not abstracted by His108) and thus the ligand was positively charged overall. In both positions, resveratrol did not retain the proton on its hydroxyl group that is favored for deprotonation, leading to an overall negative charge.

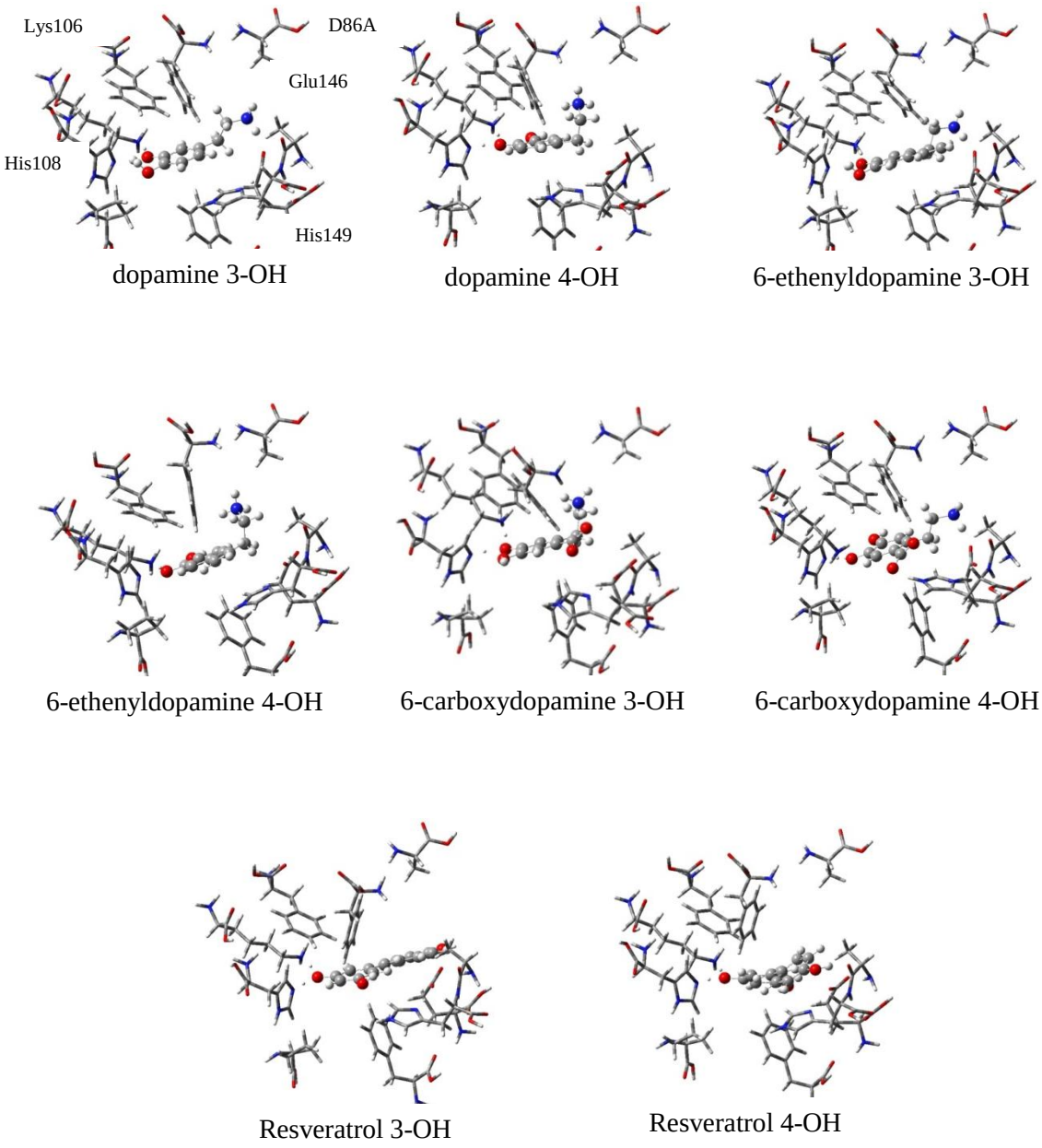

Figure 14. Optimized structures (solvated-relaxed) (M062x/6-31G) of four ligands with both 3-OH and 4-OH positioned for deprotonation in the D86A mutant active site.

The data in Table 5, column 2 show results for the D86A mutant with the ligands in each orientation. After the mutation of Asp86 to alanine, dopamine and 6-ethenyldopamine in both orientations showed weaker total interaction energies as compared to previous

calculations for the wt active site, shown in Table 5, column 1. For instance, dopamine in the 3-OH orientation was previously calculated to have a total interaction energy of -178 kcal/mol, while the energy after mutation was calculated to be -63.8 kcal/mol. In an examination of the individual amino acid-ligand interaction energies, presented in Table A4, it becomes clear that the mutation of Asp86 is the major factor in the weaker interaction. In the wt active site, the Asp86-ligand interaction was found to be -116 kcal/mol. After the mutagenesis, the Ala86-ligand interaction was 1.64 kcal/mol. The other individual residue-ligand interactions remained comparable with previously calculated data for the wt SULT1A3 active site. This observation is consistent in dopamine and 6-ethenyldopamine in both orientations. After the D86A mutation, the total interaction energies of 6-carboxydopamine remained similar to previously calculated energies for the wt active site. The lack of a significant change in 6-carboxydopamine with the D86A mutation is likely due to the initial optimization of this ligand with a negative substituent in the wt active site. In the wt active site (see previous work[1]), the negatively-charged carboxyl substituent influenced the optimization so that the amino tail was not extended as closely to the Asp86. Further, because 6-carboxydopamine had an overall neutral charge, there was less of an interaction with the negatively charged amino acid residues within the active site. Thus, after the D86A mutation, the total interaction energies were not significantly affected. After mutation, the total interaction energies of resveratrol in both orientations became stronger. The Ala86-ligand interaction for the 3-OH orientation of resveratrol was -1.42 kcal/mol, a stronger attraction than the repulsion of the Asp86-ligand complex of 31.2 kcal/mol. The

mutated amino acid accounts for the major difference between the total interaction energies.

The optimized structures of bound ligands within the active site with the E146A mutation are shown in Figure 15. Of the dopaminergic ligands, dopamine and 6-carboxydopamine retained the third proton on their amino tail, in both the 3-OH and 4-OH optimizations, leading to a local positive charge. In the case of 6-ethenyldopamine, in both optimizations, the third proton from the amino tail was abstracted by Asp86. Resveratrol became negatively after both optimizations.

Table 5, column 3 shows the total interaction energy calculations for the E146A mutation and each of the ligands in both deprotonation orientations. The interaction energies in comparison to column 1 exhibit minor changes or stronger attractive forces after the mutation. Dopamine in the 3-OH position shows an increase in the strength of the interaction energy in comparison to the calculation of the wt site, -229 kcal/mol as opposed to -178 kcal/mol. This increase can be attributed to the change in the His149-ligand interaction energy. In the normal active site, the charge of dopamine is positive, because it retains all three protons, resulting in a charged amino tail and two hydroxyl groups. This creates a less attractive force between His149, which is positively-charged, and the ligand. After the mutation E146A, dopamine is neutral and thus presents a stronger interaction with His149. This is shown through the His149-ligand energy of 43.7 kcal/mol in the wt active site and the energy of -5.31 in the mutated active site. 6-Ethenyldopamine in the 3-position favored for deprotonation showed a weaker interaction compared with the wt active site. After optimization, 6-ethenyldopamine in the 4-position is negatively-charged, since it did not retain the proton on the amino tail or

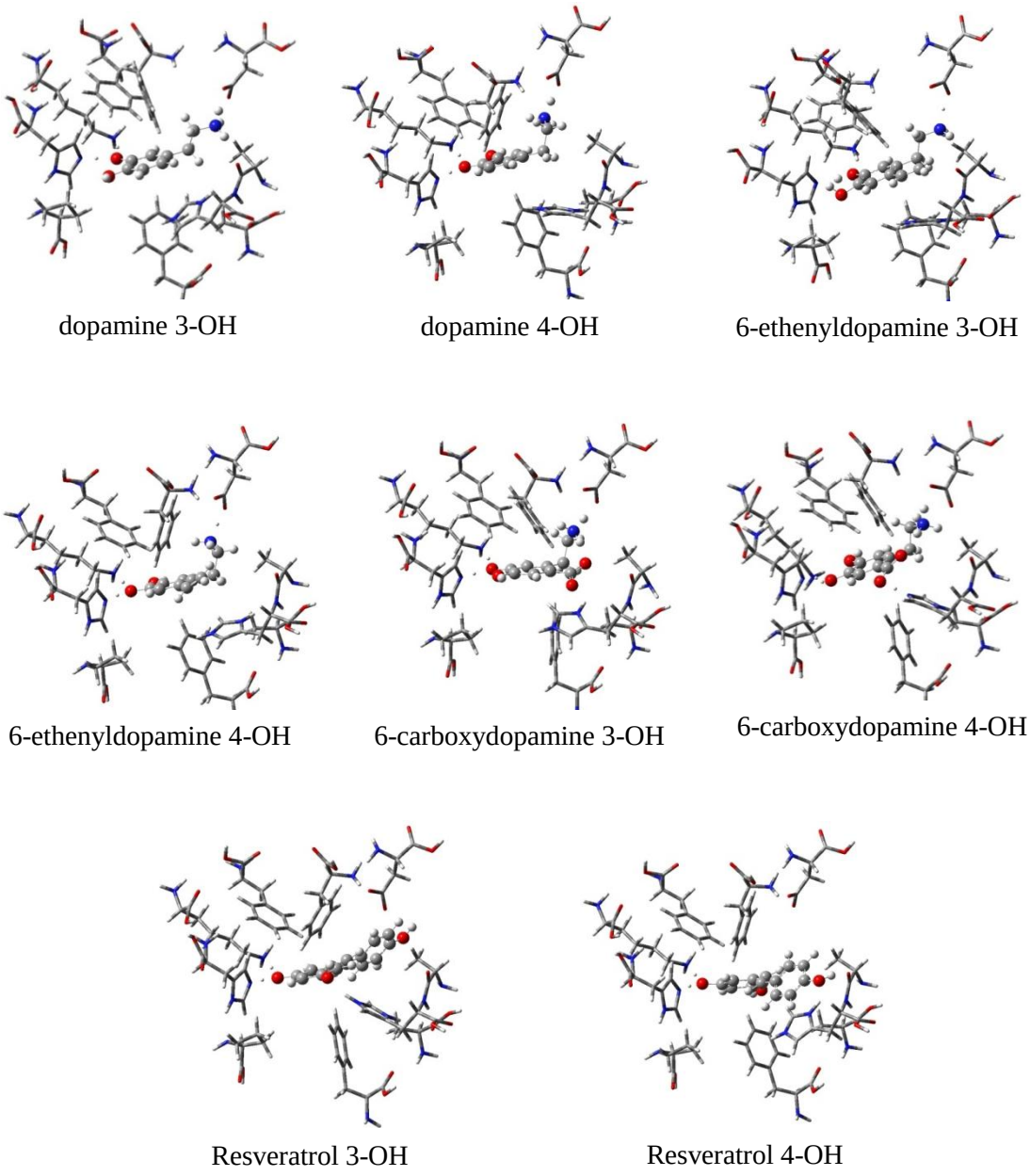

Figure 15. Optimized structures (solvated-relaxed) (M062x/6-31G) of four ligands with both 3-OH and 4-OH positioned for deprotonation in the E146A mutant active site.

on the hydroxyl group. This conformer had an interaction energy comparable to that of resveratrol. The 4-position of 6-ethenyldopamine showed a significant increase in the

interaction energy when compared with the wt calculations. As in the case of the D86A mutation, the E146A mutation resulted in a stronger attractive force between 6-carboxydopamine and the active site in comparison with energies for the wt active site with this ligand. Also, as in the D86A mutation, a stronger attractive force can be seen in the interaction energies of resveratrol in both orientations. This increase in interaction energy was predicted since the mutation of the charged aspartic acid residue made the SULT1A3 active site more similar to the SULT1A1 active site and it is known that resveratrol is preferentially bound to SULT1A1.[8]

The optimized structures of the ligand within the active site of the double mutant, where there were substitutions at D86A and E146A, making the active site more similar to SULT1A1 were determined (Figure 16). In these optimizations, all of the dopaminergic molecules retain a positively-charged amino tail. Further, all the dopaminergic molecules with the 3-position favored for deprotonation were overall positively-charged within the active site after optimization. Resveratrol became negatively-charged within the active site when oriented in both positions. In comparison with the wt and D86A, it can be noted that the amino tail is not extended toward the back of the active site in the double mutant. This change is due to the lack of a negative charge in this region of the active site since the two negatively-charged residues Asp86 and Glu146 were changed to become neutral.

The interaction energy data for ligands in the double mutant D86A/E146A active site is shown in Table 5, column 4. This data presents a similar trend to that found in column 2, the D86A mutant. Compared to column 1, dopamine and 6-ethenyldopamine in both orientations show weaker interactions with the mutated active site than with the wild type

active site. In the case of 6-carboxydopmaine, the total interaction energies in both orientations were comparable in the wt active site, as well as in both singly mutated active sites. Again, this similar total interaction energy is predicted to be due to the lack of significant attraction between 6-carboxydopamine with the Asp86 or Glu146 residues in the wt SULT1A3 active site. As in columns 2 and 3, resveratrol in both orientations was found to have stronger total interaction energies after the mutations of both D86A and E146A. Resveratrol showed the most negative and thus most attractive interaction energies when both mutations occurred, which resulted in a more similar active site to SULT1A1.

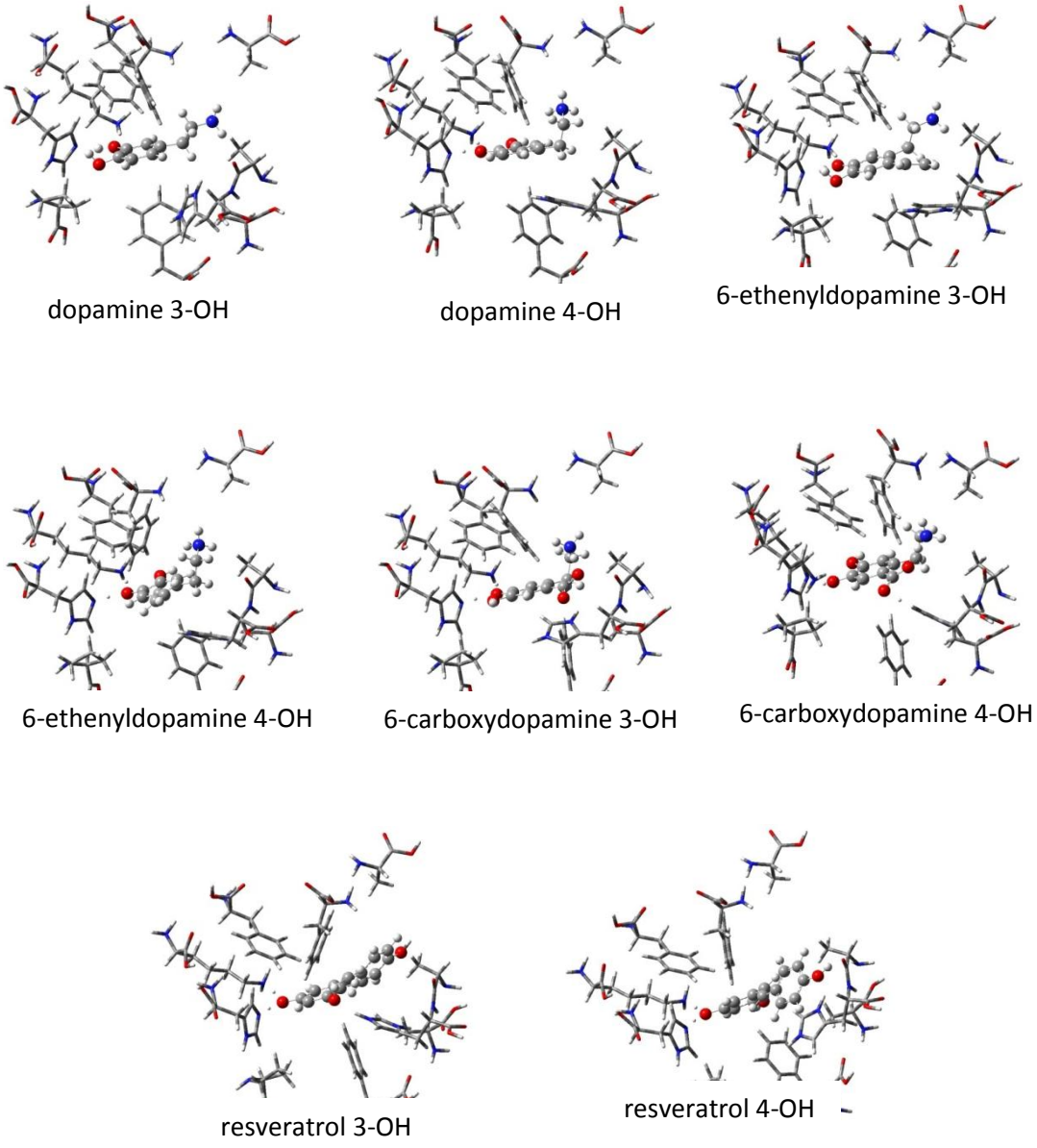

Figure 16. Optimized structures (solvated-relaxed) (M062x/6-31G) of four ligands with both 3-OH and 4-OH positioned for deprotonation in the D86A + E146A mutant active site.

3.4 Salbutamol

All four orientations of salbutamol optimized with the relaxed-solvated model within the SULT1A3 active site are shown in Figure 17.[25] In all optimizations, salbutamol retained

the protons on the benzylic and phenolic alcohols. To be consistent with previous work, the 3-OH and 4-OH terminology is being used (see Figure 16). The protons were thus not abstracted by the amino residue, His108. The positioning of salbutamol in the 3-OH and 4-OH positions is more favorably situated within the active site than salbutamol in the "flipped" orientation (indicated by salbutamol').

The interaction energies between salbutamol and five significant amino acid residues within the active site—His108, Lys106, Asp86, Glu146, and His149 were calculated (Table 6). In all optimizations of salbutamol, the ligand retains its protons and thus is positively-charged. Therefore, there is a strong attractive interaction between salbutamol and the negatively charged residues, Asp86 and Glu146. In this study, negative interaction energies indicate an attractive force between the ligand and the active site and positive interaction energies indicate a repulsive force.

Table 6. Counterpoise-corrected MP2 and M062X interaction energies of salbutamol in each orientation optimized in the solvated-relaxed model.[1] Salbutamol' refers to the ligand in a flipped orientation. Energies in kcal/mol.

		His108	Lys106	Asp86	Glu146	His149	Total
Salbutamol 3-OH	MP2	-15.7	22.4	-104	-93.9	42.6	-168
	M062X	-17.6	19.4	-109	-96.7	42.9	-181
Salbutamol 4-OH	MP2	-16.2	13.9	-55.7	-74.4	53.3	-96.9
	M062X	-18.9	10.7	-55.4	-74.5	53.2	-107
Salbutamol' 3-OH	MP2	-15.9	27.2	-60.8	-102	54.6	-113
	M062X	-18.5	24.7	-60.3	-105	53.8	-125
Salbutamol' 4-OH	MP2	-7.97	18.6	-38.2	-50.5	39.5	-66.5
	M062X	-9.83	15.3	-38.0	-50.8	39.8	-73.1

The optimized salbutamol 3-OH and salbutamol' 3-OH were oriented in a way to favor deprotonation at the benzylic alcohol on the ligand. In these orientations, the tail of salbutamol is extended in such a way to allow for favorable interactions with Asp86 within the active site. The interaction energy between salbutamol 3-OH and Asp86 is -104 (kcal/mol), a more favorable interaction than the energy between salbutamol 4-OH and Asp86 is -55.7 (kcal/mol). Similarly, there are more favorable interaction energies between salbutamol in the 3-OH position and Glu146. The interaction energy between salbutamol 3-OH and Glu146 is –93.9 (kcal/mol), a more favorable interaction than the energy between salbutamol 4-OH and Glu146 is -74.4 (kcal/mol).

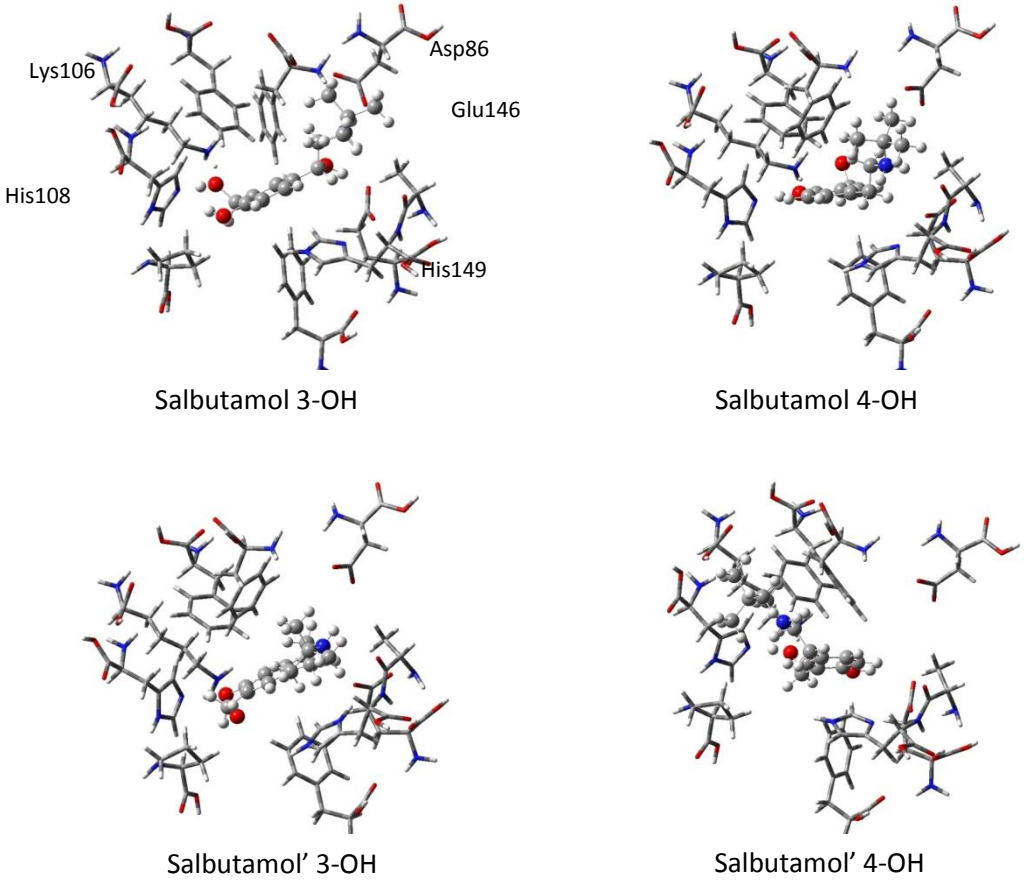

Figure 17. Optimized structures (M062x/6-31G) of salbutamol in all four orientations. Optimizations were performed with non-rigid amino acid residues and implicit solvation.

The individual interaction energies between the positively charged amino acid residues with salbutamol in all orientations exhibit a repulsive force. In the case of salbutamol 3-OH, the interaction with Lys106 is 22.4 (kcal/mol) and the interaction with His149 is 42.6 (kcal/mol) (Table A4). Salbutamol' 3-OH exhibits the most repulsive force with an interaction with Lys106 of 27.2 (kcal/mol) and with His149, 54.6 (kcal/mol). In the other three orientations of salbutamol there is a similar trend of repulsive interactions with these positively charged residues.

When salbutamol is positioned in a way that favors deprotonation at the 4-OH position, there is a favorable interaction energy, although not as strongly attractive as when the molecule is positioned to favor the 3-OH position. Again, in the case of salbutamol 4-OH, there is an attractive force between the ligand and the SULT1A3 active site of -96.9 (kcal/mol). The "flipped" orientation also shows a favorable interaction of -66.5 (kcal/mol) but is the least suitable position based on the calculated interaction energies.

The total interaction energy for dopamine in the active site was calculated to be -178 (kcal/mol). Thus, salbutamol shows a favorable interaction energy, but calculations suggest that it has less of an affinity for the SULT1A3 active site than dopamine. This trend agrees with experimental data in the study by Ko, *et al.*[15]

All interaction energy calculations showed a favorable interaction between salbutamol and the SULT1A3 active site.

3. Conclusions

3.1 Model Chemistries

The more realistic model presented here, the solvated-relaxed model, shows considerable differences from the two other models, showing that the effects of solvation and relaxation of the active site residuesare significant. The effect of solvation is large, taking the average interaction energy from -116 kcal/mol to -173 kcal/mol, though the effect of relaxing the active site and including solvation is more significant, taking the average interaction energy to -252 kcal/mol. 6-Carboxydopamine has the most strongly binding interaction energy of the ligands studied here in the SX model. This is due to the negative charge on the ligand's carboxyl group creating binding interactions with the positively-charged lysine and histidine residues in the active site. Three other ligands, 6-cyanodopamine, 6-hydroxydopamine, and 6-bromodopamine also have stronger interaction energies than the endogenous ligand dopamine. The more hydrophobic ligands (nitrodopamine, ethenyldopamine, dihydroxybenzonitrile, (dihydroxyphenyl)acetonitrile, and resveratrol) bind less strongly than dopamine. The ligands lacking the positively charged amino tail show less favorable binding energy than the dopaminergic ligands in the SX model. This is in keeping with experimental results; in particular, it is known that resveratrol is selected by SULT1A1 rather than SULT1A3[11], and that is reflected in the low interaction energy shown here.[27]

In work from 2007, Yasuda, *et al*. found K_m values for dopamine and 6-hydroxydopamine in SULT1A3 of 7.0 and 19.4 μmol/L, suggesting that dopamine has considerably more affinity for SULT1A3 than 6-hydroxydopamine.[28] In the current work, the VR model shows dopamine and 6-hydroxydopamine to have near-equal interaction energies with SULT1A3. The SR model, however, shows that dopamine has a much higher interaction energy than 6-hydroxydopamine, in agreement with the

experimental data. However, the SX model reverses the order and has a stronger interaction for 6-hydroxydopamine. Unlike the data presented here, the experimental K_m values were not for a specific position of sulfation, which, along with the limited experimental values make a correlation with the computational data complicated. A larger number of compounds with corresponding kinetic data are needed to determine which model best describes the experimental data.. Finally, the work of Miksits, *et al.* present a value for K_m of resveratrol in SULT1A1 of 29.2 μmol/L; while this is not comparable to the current SULT1A3 values, the literature suggests that the K_m value would be *higher* in SULT1A3, and any value higher than 29.2 μmol/L would correlate well (compared to dopamine and 6-hydroxydopamine) in the VR and SX models, however not in the SR model.[29]

3.2 pKa

Relative pK_a values can be used to suggest how easily the proton will be abstracted from the hydroxyl group of the ligand. The study by Yasuda, *et al*., presents values for V_{max} for both ligands, which may be correlated with our calculated pK_a values, assuming that deprotonation is part of a rate-determining process in the sulfation reaction. The V_{max} values of 68.1 and 37.4 nmol/min/mg for dopamine and 6-hydroxydopamine, respectively, do correlate well with our calculated pK_a values of 3.2 and 3.6 (for the two molecules, deprotonated on the 3-position) and 2.8 and 3.02 (for the two dopamine molecules, deprotonated on the 4-position).[28]

3.3 Point Mutations

The computational site-directed mutagenesis of E146A agrees with experimental data for dopamine.[4,7] SULT1A3 showed less affinity for dopamine following the D86A mutation

and with both E146A and D86A mutations. The mutation of the active site at these positions results in an active site similar to SULT1A1, which exhibits a weaker affinity for dopaminergic molecules.[4,7] 6-Ethenyldopamine also exhibited a similar trend to dopamine in its total interaction energies, except in the E146A mutant with the 4-position favored for deprotonation.

The interaction energies of 6-carboxydopamine showed an increase with each site-directed mutagenesis calculation. Because of the negatively charged carboxyl substituent and the neutral overall charge of the molecule, the interaction with the charged residues was not as favorable. Therefore when these sites where changed to an uncharged species, the total interaction energy of 6-carboxydopamine for the mutated SULT1A3 exhibited a stronger affinity.

All calculations with a mutated active site resulted in an increase in interaction energy, and thus predicted affinity, of resveratrol with the SULT1A3 active site. The ligand became negatively-charged in all the mutant optimizations. The optimization and calculations for the SULT1A3 optimization with E146A and D86A mutations showed the greatest affinity for resveratrol. These results were consistent with predictions based on the nature of the SULT1A1 and SULT1A3 enzymes.[8]

3.4 Salbutamol

Calculated energies for salbutamol indicate that this molecule has favorable interactions with the residues in the SULT1A3 active site. The strongest interaction energy of -168 kcal/mol suggests that salbutamol at the 3-OH position is favored for deprotonation.

In line with other work, these findings suggest that the 3-OH would be the more favorable product for sulfation, although experimental work suggests that the sulfation of the 4-OH is more likely.[15] This contrast would suggest that the binding energy between the ligand and the active site is not the major factor in the selectivity of sulfation of salbutamol, catalyzed by SULT1A3.

Salbutamol in all orientations shows favorable interactions with SULT1A3, although less strong than the attractive forces between the endogenous compound, dopamine, and the active site.

4. References

1. Gamage, N.; Barnett, A.; Hempel, N.; Duggleby, R. G.; Windmill, K. F.; Martin, J. L.; McManus, M. E., Human Sulfotransferases and their Role in Chemical Metabolism. *Toxicological Sciences* **2006,** *90* (1), 5-22.

2. Dajani, R.; Cleasby, A.; Neu, M.; Wonacott, A. J.; Jhoti, H.; Hood, A. M.; Modi, S.; Hersey, A.; Taskinen, J.; Cooke, R. M.; Manchee, G. R.; Coughtrie, M. W. H., X-ray crystal structure of human dopamine sulfotransferase, SULT1A3: Molecular modeling and quantitative structure-activity relationship analysis demonstrate a molecular basis for sulfotransferase substrate specificity. *Journal of Biological Chemistry* **1999,** *274* (53), 37862-37868.

3. Sidharthan Neelima, P.; Minchin Rodney, F.; Butcher Neville, J., Cytosolic sulfotransferase 1A3 is induced by dopamine and protects neuronal cells from dopamine toxicity: role of D1 receptor-N-methyl-D-aspartate receptor coupling. *The Journal of biological chemistry* **2013,** *288* (48), 34364-74.

4. Lu, J.-H.; Li, H.-T.; Liu, M.-C.; Zhang, J.-P.; Li, M.; An, X.-M.; Chang, W.-R., Crystal structure of human sulfotransferase SULT1A3 in complex with dopamine and 3'-phosphoadenosine 5'-phosphate. *Biochemical and Biophysical Research Communications* **2005,** *335* (2), 417-423.

5. Itaaho, K.; Alakurtti, S.; Yli-Kauhaluoma, J.; Taskinen, J.; Coughtrie Michael, W. H.; Kostiainen, R., Regioselective sulfonation of dopamine by SULT1A3 in vitro provides a molecular explanation for the preponderance of dopamine-3-O-sulfate in human blood circulation. *Biochem Pharmacol* **2007,** *74* (3), 504-10.

6. Yamamoto, T.; Yamatodani, A.; Nishimura, M.; Wada, H., Determination of dopamine-3- and -4-O-sulfate in human plasma and urine by anion-exchange high-performance liquid chromatography with fluorimetric detection. *Journal of Chromatography, Biomedical Applications* **1985,** *342* (2), 261-7.

7. Strobel, G.; Werle, E.; Weicker, H., Isomer specific kinetics of dopamine β-hydroxylase and arylsulfatase towards catecholamine sulfates. *Biochemistry International* **1990,** *20* (2), 343-51.

8. Bian, H. S.; Ngo, S. Y. Y.; Tan, W.; Wong, C. H.; Boelsterli, U. A.; Tan, T. M. C., Induction of human sulfotransferase 1A3 (SULT1A3) by glucocorticoids. *Life Sciences* **2007,** *81* (25-26), 1659-1667.

9. Zhao, Y.; Truhlar, D. G., Density Functionals for Noncovalent Interaction Energies of Biological Importance. *Journal of Chemical Theory and Computation* **2007,** *3* (1), 289-300.

10. Hohenstein, E. G.; Chill, S. T.; Sherrill, C. D., Assessment of the Performance of the M05-2X and M06-2X Exchange-Correlation Functionals for Noncovalent Interactions in Biomolecules. *Journal of Chemical Theory and Computation* **2008,** *4* (12), 1996-2000.

11. Miksits, M.; Wlcek, K.; Svoboda, M.; Thalhammer, T.; Ellinger, I.; Stefanzl, G.; Falany, C. N.; Szekeres, T.; Jaeger, W., Expression of sulfotransferases and sulfatases in human breast

cancer: Impact on resveratrol metabolism. *Cancer Letters (Shannon, Ireland)* **2010,** *289* (2), 237-245.

12. Ozawa, S.; Nagata, K.; Shimada, M.; Ueda, M.; Tsuzuki, T.; Yamazoe, Y.; Kato, R., Primary structures and properties of two related forms of aryl sulfotransferases in human liver. *Pharmacogenetics* **1995,** *5* (Spec. Issue, ,Spec. Issue), S135-S140.

13. Blanchard, R. L.; Freimuth, R. R.; Buck, J.; Weinshilboum, R. M.; Coughtrie, M. W. H., A proposed nomenclature system for the cytosolic sulfotransferase (SULT) superfamily. *Pharmacogenetics* **2004,** *14* (3), 199-211.

14. Jacobson, G. A.; Yee, K. C.; Wood-Baker, R.; Walters, E. H., SULT 1A3 single-nucleotide polymorphism and the single dose pharmacokinetics of inhaled salbutamol enantiomers: Are some athletes at risk of higher urine levels? *Drug Testing and Analysis* **2015,** *7* (2), 109-113.

15. Ko, K. A.; Kurogi, K.; Davidson, G.; Liu, M.-Y.; Sakakibara, Y.; Suiko, M.; Liu, M.-C., Sulfation of ractopamine and salbutamol by the human cytosolic sulfotransferases. *Journal of Biochemistry* **2012,** *152* (3), 275-283.

16. Brix, L. A.; Barnett, A. C.; Duggleby, R. G.; Leggett, B.; McManus, M. E., Analysis of the Substrate Specificity of Human Sulfotransferases SULT1A1 and SULT1A3: Site-Directed Mutagenesis and Kinetic Studies. *Biochemistry* **1999,** *38* (32), 10474-10479.

17. DiGiovanni, K. M.; Katherine Hatstat, A.; Rote, J.; Cafiero, M., MP2//DFT calculations of interaction energies between acetaminophen and acetaminophen analogues and the aryl sulfotransferase active site. *Computational & Theoretical Chemistry* **2013,** *1007*, 41-47.

18. Tsuzuki, S.; Honda, K.; Uchimaru, T.; Mikami, M.; Tanabe, K., Origin of Attraction and Directionality of the π/π Interaction: Model Chemistry Calculations of Benzene Dimer Interaction. *Journal of the American Chemical Society* **2002,** *124* (1), 104-112.

19. Tomasi, J.; Mennucci, B.; Cammi, R., Quantum Mechanical Continuum Solvation Models. *Chemical Reviews (Washington, DC, United States)* **2005,** *105* (8), 2999-3093.

20. Christopher J. Cramer* and Donald G. Truhlar. Implicit Solvation Models: Equilibria, Structure, Spectra, and Dynamics, Chem. Rev. **1999**, 99, 2161-2200.

21. Kevin E. Riley, Jiři Vondrášeka and Pavel Hobza. Performance of the DFT-D method, paired with the PCM implicit solvation model, for the computation of interaction energies of solvated complexes of biological interest. Phys. Chem. Chem. Phys., **2007**,9, 5555-5560.

22. Gaussian 09, Revision **C.01**, M. J. Frisch, G. W. Trucks, H. B. Schlegel, G. E. Scuseria, M. A. Robb, J. R. Cheeseman, G. Scalmani, V. Barone, B. Mennucci, G. A. Petersson, H. Nakatsuji, M. Caricato, X. Li, H. P. Hratchian, A. F. Izmaylov, J. Bloino, G. Zheng, J. L. Sonnenberg, M. Hada, M. Ehara, K. Toyota, R. Fukuda, J. Hasegawa, M. Ishida, T. Nakajima, Y. Honda, O. Kitao, H. Nakai, T. Vreven, J. A. Montgomery, Jr., J. E. Peralta, F. Ogliaro, M. Bearpark, J. J. Heyd, E. Brothers, K. N. Kudin, V. N. Staroverov, R. Kobayashi, J. Normand, K. Raghavachari, A. Rendell, J. C. Burant, S. S. Iyengar, J. Tomasi, M. Cossi, N. Rega, J. M. Millam, M. Klene, J.

E. Knox, J. B. Cross, V. Bakken, C. Adamo, J. Jaramillo, R. Gomperts, R. E. Stratmann, O. Yazyev, A. J. Austin, R. Cammi, C. Pomelli, J. W. Ochterski, R. L. Martin, K. Morokuma, V. G. Zakrzewski, G. A. Voth, P. Salvador, J. J. Dannenberg, S. Dapprich, A. D. Daniels, Ö. Farkas, J. B. Foresman, J. V. Ortiz, J. Cioslowski, and D. J. Fox, Gaussian, Inc., Wallingford CT, **2009**.

23. Zhang, S; Baker, J; Pulay, P., Reliable and Efficient First Principles-Based for Predicting pKa Values. 1. Methodology. J. Phys. Chem. A. **2010,** 114:425-431.

24. Zlatovic, M. V.; Sukalovic, V. V.; Roglic, G. M.; Kostic-Rajacic, S. V.; Andric, D. B., The influence of dispersive interactions on the binding affinities of ligands with an arylpiperazine moiety to the dopamine D2 receptor. *Journal of the Serbian Chemical Society* **2009,** *74* (10), 1051-1061.

24. Bigler, D. J.; Peterson, L. W.; Cafiero, M., Effects of implicit solvent and relaxed amino acid side chains on the MP2 and DFT calculations of ligand-protein structure and electronic interaction energies of dopaminergic ligands in the SULT1A3 enzyme active site. *Computational & Theoretical Chemistry* **2015,** *1051*, 79-92.

25. Sinnokrot, M. O.; Sherrill, C. D., High-Accuracy Quantum Mechanical Studies of Ï€-Ï€ Interactions in Benzene Dimers. *Journal of Physical Chemistry A 110* (37), 10656-10668.

26. Walle, T.; Hsieh, F.; DeLegge, M. H.; Oatis, J. E., Jr.; Walle, U. K., High absorption but very low bioavailability of oral resveratrol in humans. *Drug Metabolism & Disposition* **2004,** *32* (12), 1377-1382.

27. Yasuda, S.; Liu, M.-Y.; Suiko, M.; Sakakibara, Y.; Liu, M.-C., Hydroxylated serotonin and dopamine as substrates and inhibitors for human cytosolic SULT1A3. *Journal of Neurochemistry* **2007,** *103* (6), 2679-2689.

28. Miksits, M.; Maier-Salamon, A.; Aust, S.; Thalhammer, T.; Reznicek, G.; Kunert, O.; Haslinger, E.; Szekeres, T.; Jaeger, W., Sulfation of resveratrol in human liver: Evidence of a major role for the sulfotransferases SULT1A1 and SULT1E1. *Xenobiotica* **2005,** *35* (12), 1101-1119.

5. Appendix

Table 4: Counterpoise-corrected MP2 and M062X calculations of the interaction energies of the ligands optimized *in vacuo* and with rigid amino acid residues (vacuum-rigid, VR model). Energies in kcal/mol.[22]

		His108	Lys106	Asp86	Glu146	His149	Total
Dopamine 3-OH	MP2	-18.9	34.1	-111	-8.69	-4.50	-118
	M062X	-21.7	31.7	-116	-8.47	-3.91	-126
Dopamine 4-OH	MP2	-12.4	-21.3	-18.4	-1.51	-1.44	-60.4
	M062X	-14.6	-25.7	-21.6	-2.35	-1.06	-69.2
6-hydroxydopamine 3-OH	MP2	-10.8	-13.3	-15.7	-5.40	-0.81	-53.3
	M062X	-13.7	-15.8	-19.5	-6.24	-1.39	-62.8
6-hydroxydopamine 4-OH	MP2	-15.7	28.2	-116	-5.67	-5.92	-125
	M062X	-16.5	24.8	-120	-6.33	-5.32	-133
1,2,3,4-tetrahydroisoquinoline-6,7-diol 3-OH	MP2	-8.32	31.5	-98.8	-8.11	-4.08	-95.0
	M062X	-8.10	30.0	-102	-7.99	-3.42	-97.6
1,2,3,4-tetrahydroisoquinoline-6,7-diol 4-OH	MP2	-15.5	23.9	-48.9	2.51	-7.45	-60.1
	M062X	-16.6	21.0	-48.7	0.51	-7.82	-66.6
6-nitrodopamine 3-OH	MP2	-102	-107	-27.0	-4.38	-1.17	-254
	M062X	-106	-111	-30.4	-4.86	-0.96	-264
6-nitrodopamine 4-OH	MP2	-13.1	-17.5	-0.287	-1.82	-4.65	-43.2
	M062X	-15.1	-20.4	-0.148	-3.39	-5.25	-49.3
6-bromodopamine 3-OH	MP2	-11.6	-10.0	-20.9	-2.88	-0.46	-53.0
	M062X	-15.4	-12.6	-24.3	-1.09	-0.28	-62.8
6-bromodopamine 4-OH	MP2	-17.2	21.8	-51.5	-6.39	-9.95	-77.2
	M062X	-18.6	18.9	-51.4	-8.82	-12.9	-89.9
6-cyanodopamine 3-OH	MP2	-13.1	-7.59	-17.4	-1.61	0.0200	-48.2
	M062X	-17.1	-9.53	-21.3	-2.09	0.550	-56.7

6-cyanodopamine 4-OH	MP2	-106	-118	-23.2	-4.57	-2.51	-264
	M062X	-110	-125	-26.3	-5.83	-2.47	-278
6-ethenyldopamine 3-OH	MP2	-8.98	-13.5	-19.7	-2.64	-1.26	-55.1
	M062X	-12.6	-15.5	-23.0	-3.45	-1.27	-64.1
6-ethenyldopamine 4-OH	MP2	-12.7	-21.7	-17.9	-1.93	-1.34	-62.2
	M062X	-14.7	-26.0	-20.9	-3.42	-1.17	-71.1
6-carboxydopamine 3-OH	MP2	-10.4	-20.5	-55.6	-13.4	1.00	-106
	M062X	-5.95	-16.7	-59.1	-11.1	1.82	-99.1
6-carboxydopamine 4-OH	MP2	-8.20	-24.0	-58.4	-15.8	-39.5	-156
	M062X	-8.57	-28.2	-61.3	-16.1	-42.3	-168
3,4-dihydroxybenzonitrile	MP2	-13.9	-6.45	1.96	-0.487	-1.25	-27.1
	M062X	-16.5	-8.69	2.22	-0.704	-0.828	-29.8
3,4-dihydroxybenzonitrile	MP2	-11.8	-14.4	-4.70	-1.42	0.939	-36.3
	M062X	-14.4	-17.4	-4.55	-1.48	1.17	-40.9
2-(3,4-dihydroxyphenyl)	MP2	-4.95	-20.1	-11.0	-1.53	-1.07	-42.4
acetonitrile	M062X	-0.670	-22.0	-13.7	-1.18	-0.670	-46.3
2-(3,4-dihydroxyphenyl)	MP2	-9.75	-19.2	1.04	2.27	-2.16	-32.7
acetonitrile	M062X	-11.6	-22.8	1.37	1.54	-1.83	-38.2
Resveratrol 3-OH	MP2	-9.60	-16.0	-9.46	-2.39	-3.31	-48.8
	M062X	-11.6	-18.7	-10.9	-1.67	-3.11	-51.6
Resveratrol 5-OH	MP2	-10.3	-17.8	-2.47	-4.24	-3.05	-48.3
	M062X	-11.6	-21.3	-2.18	-3.93	-4.10	-55.8

Table 5: Counterpoise-corrected MP2 and M062X calculations of the interaction energies of the ligands optimized with implicit water solvation and with rigid amino acid residues (solvated-rigid, SR model). Energies in kcal/mol.[22]

		His108	Lys106	Asp86	Glu146	His149	Total
Dopamine 3-OH	MP2	-18.8	33.9	-105	-9.46	-4.65	-112
	M062X	-22.0	31.9	-108	-9.30	-4.05	-119
Dopamine 4-OH	MP2	-60.5	-68.0	-58.1	-5.30	-3.89	-202
	M062X	-63.5	-75.0	-62.2	-6.29	-3.45	-215
6-hydroxydopamine 3-OH	MP2	-19.7	37.5	-109	-9.96	-1.92	-112
	M062X	-22.8	35.4	-113	-11.0	-2.21	-121
6-hydroxydopamine 4-OH	MP2	-20.6	32.4	-113	-4.60	-5.31	-121
	M062X	-22.8	29.0	-117	-5.00	-4.60	-129
1,2,3,4-tetrahydroisoquinoline-6,7-diol 3-OH	MP2	-10.5	33.8	-96.5	-7.30	-3.75	-92.2
	M062X	-10.6	31.9	-99.2	-7.19	-3.10	-94.4
1,2,3,4-tetrahydroisoquinoline-6,7-diol 4-OH	MP2	-17.5	25.1	-44.7	2.77	-8.28	-55.4
	M062X	-19.9	21.9	-44.6	1.84	-10.1	-62.9
6-nitrodopamine 3-OH	MP2	-51.9	-49.2	-54.2	-7.44	-1.15	-172
	M062X	-54.8	-52.5	-58.6	-8.30	-0.573	-180
6-nitrodopamine 4-OH	MP2	-45.3	-46.4	-61.4	-5.16	-3.95	-170
	M062X	-46.7	-51.4	-65.4	-6.33	-3.16	-180
6-bromodopamine 3-OH	MP2	-71.7	-65.4	-56.8	-6.11	-2.58	-210
	M062X	-67.4	-70.5	-60.8	-8.39	-2.54	-216
6-bromodopamine 4-OH	MP2	-18.2	22.4	-49.9	-5.24	-10.4	-76.3
	M062X	-20.3	19.4	-50.0	-7.66	-13.1	-88.4

6-cyanodopamine 3-OH	MP2	-56.1	-59.1	-57.7	-10.1	-2.06	-192
	M062X	-59.1	-63.3	-61.3	-10.7	-1.42	-201
6-cyanodopamine 4-OH	MP2	-51.4	-57.8	-62.0	-6.26	-2.85	-187
	M062X	-53.7	-64.2	-66.8	-7.48	-2.42	-199
6-ethenyldopamine 3-OH	MP2	--17.6	35.9	-108	-6.59	-3.27	-108
	M062X	-21.4	34.2	-112	-7.42	-3.05	-118
6-ethenyldopamine 4-OH	MP2	-57.5	-66.7	-58.4	-5.72	-3.30	-199
	M062X	-59.9	-73.7	-62.5	-7.32	-3.12	-212
6-carboxydopamine 3-OH	MP2	-115	-120	7.51	-9.49	-1.84	-256
	M062X	-120	-125	4.26	-9.86	-2.10	-269
6-carboxydopamine 4-OH	MP2	-10.4	-23.7	-52.1	-13.7	-4.94	-115
	M062X	-12.0	-27.1	-54.7	-14.0	-4.62	-122
3,4-dihydroxybenzonitrile	MP2	-13.2	-7.34	5.41	0.287	-1.06	-24.2
	M062X	-16.8	-8.92	5.75	0.632	-0.716	-26.8
3,4-dihydroxybenzonitrile	MP2	-111	-113	36.4	-4.64	-1.48	-203
	M062X	-115	-117	36.5	-4.78	-1.32	-213
2-(3,4-dihydroxyphenyl) acetonitrile	MP2	-10.9	-15.2	2.51	-1.33	-2.15	-35.4
	M062X	-14.9	-17.4	2.65	-0.934	-1.77	-39.9
2-(3,4-dihydroxyphenyl) acetonitrile	MP2	-10.7	-19.1	3.56	1.58	-2.17	-32.9
	M062X	-13.2	-22.4	3.86	1.44	-1.89	-37.9
Resveratrol 3-OH	MP2	-10.5	-15.4	-7.92	-2.57	-2.65	-47.6
	M062X	-13.3	-17.8	-8.51	-2.17	-2.16	-50.2
Resveratrol 5-OH	MP2	-101	-125	39.5	-6.70	-5.11	-214
	M062X	-103	-133	39.6	-6.79	-6.37	-227

Table 6: Counterpoise-corrected MP2 and M062X calculations of the interaction energies of the ligands optimized in implicit water solvation and with relaxed amino acid residues (solvated-relaxed, SX model). Energies in kcal/mol. [22]

		His108	Lys106	Asp86	Glu146	His149	Total
Dopamine 3-OH	MP2	-18.3	30.9	-116	-105	43.7	-178
	M062X	-21.8	29.1	-121	-108	44.0	-189
Dopamine 4-OH	MP2	-67.6	-70.1	-73.1	-20.0	-5.82	-246
	M062X	-72.2	-76.0	-80.0	-21.3	-5.04	-263
6-hydroxydopamine 3-OH	MP2	-18.8	36.0	-115	-113	38.5	-183
	M062X	-21.9	33.8	-119	-118	38.2	-196
6-hydroxydopamine 4-OH	MP2	-66.0	-71.4	-70.9	-24.9	-9.93	-256
	M062X	-70.1	-77.2	-76.3	-26.1	-10.2	-273
1,2,3,4-tetrahydroisoquinoline-6,7-diol 3-OH	MP2	23.5	-20.1	-109	-101	48.2	-169
	M062X	22.5	-23.8	-113	-103	48.9	-178
1,2,3,4-tetrahydroisoquinoline-6,7-diol 4-OH	MP2	-62.5	-70.7	-7.47	-20.0	9.51	-169
	M062X	-67.4	-76.3	-7.43	-21.5	9.60	-180
6-nitrodopamine 3-OH	MP2	-49.7	-50.1	-63.2	-34.7	-18.1	-227
	M062X	-52.7	-53.1	-68.2	-37.7	-18.0	-239
6-nitrodopamine 4-OH	MP2	-47.6	-50.2	-67.6	-17.1	-12.1	-207
	M062X	-49.5	-55.0	-72.8	-18.0	-13.3	-220
6-bromodopamine 3-OH	MP2	-63.1	-69.7	-64.1	-43.4	-9.01	-260
	M062X	-66.8	-75.0	-68.5	-47.1	-9.89	-276
6-bromodopamine 4-OH	MP2	-15.5	-13.2	-14.1	-0.794	-0.00986	-50.9
	M062X	-17.6	-16.7	-17.1	-4.46	-0.265	-62.7
6-cyanodopamine 3-OH	MP2	-53.9	-59.9	-66.7	-41.6	-12.3	-246
	M062X	-56.8	-64.2	-71.4	-44.1	-12.6	-260

6-cyanodopamine 4-OH	MP2	-104	-116	-32.2	40.6	-56.9	-280
	M062X	-108	-122	-36.5	39.3	-57.8	-295
6-ethenyldopamine 3-OH	MP2	-16.5	34.7	-113	-99.3	39.1	-166
	M062X	-19.8	32.8	-117	-103	38.8	-178
6-ethenyldopamine 4-OH	MP2	-65.5	-69.6	-74.9	-20.1	-7.50	-248
	M062X	-69.8	-75.6	-81.6	-21.6	-7.52	-265
6-carboxydopamine 3-OH	MP2	-107	-127	9.78	56.9	-75.7	-265
	M062X	-110	-134	6.74	57.6	-77.8	-280
6-carboxydopamine 4-OH	MP2	-130	-132	-17.6	4.17	-94.2	-397
	M062X	-135	-138	-21.2	1.97	-98.0	-418
3,4-dihydroxybenzonitrile	MP2	-87.7	-110	42.3	42.8	-51.2	-175
	M062X	-90.5	-116	42.4	42.3	-50.9	-185
3,4-dihydroxybenzonitrile	MP2	-100	-114	41.0	50.5	-59.2	-195
	M062X	-103	-119	41.3	51.0	-59.8	-202
2-(3,4-dihydroxyphenyl) acetonitrile	MP2	-109	-129	39.9	35.5	-47.3	-227
	M062X	-113	-136	39.9	35.4	-47.2	-237
2-(3,4-dihydroxyphenyl) acetonitrile	MP2	-116	-123	46.0	36.6	-49.5	-220
	M062X	-121	-129	46.4	36.2	-50.0	-231
Resveratrol 3-OH	MP2	-114	-119	31.2	38.7	-59.1	-239
	M062X	-118	-125	30.5	39.3	-60.3	-250
Resveratrol 5-OH	MP2	-106	-125	39.5	39.3	-60.2	-230
	M062X	-109	-132	39.6	39.3	-60.9	-245

Table 9. Counterpoise-corrected MP2 and M062X interaction energies of ligands optimized in the solvated-relaxed model. X86 and X146 refer to the different mutants referenced in the left-hand column. wt Interaction Energies taken for comparison from previous work.[1] Energies in kcal/mol.[22]

		His108	Lys106	X86	X146	His149	Total
Dopamine 3-OH	MP2	-18.3	30.9	-116	-105	43.7	-178
Wild type	M062X	-21.8	29.1	-121	-108	44.0	-189
Dopamine 3-OH	MP2	-19.0	31.5	1.64	-109	43.6	-63.8
D86A	M062X	-22.6	29.7	1.91	-113	44.0	-71.3
Dopamine 3-OH	MP2	-70.4	-70.6	-70.2	-0.122	-5.31	-229
E146A	M062X	-75.1	-75.0	-75.4	0	-5.32	-243
Dopamine 3-OH	MP2	-13.3	32.6	2.01	-0.920	46.3	56.4
D86A, E146A	M062X	-17.0	30.7	2.28	-0.777	47.1	52.7
Dopamine 4-OH	MP2	-67.6	-70.1	-73.1	-19.9	-5.82	-246
Wild type	M062X	-72.2	-75.9	-79.9	-21.3	-5.04	-263
Dopamine 4-OH	MP2	-19.0	-70.9	1.59	-20.1	-4.00	-125
D86A	M062X	-22.6	-76.8	1.78	-21.4	-3.28	-134
Dopamine 4-OH	MP2	-69.0	-70.7	-74.5	-0.190	-5.48	-229
E146A	M062X	-73.7	-76.5	-81.2	0.0245	-4.56	-245
Dopamine 4-OH	MP2	-63.6	-71.3	1.55	-0.308	-3.86	-150
D86A, E146A	M062X	-67.8	-77.1	1.73	-0.174	-2.92	-158
6-Carboxydopamine 3-OH	MP2	-107	-127	9.78	56.9	-75.7	-265
Wild type	M062X	-110	-134	6.74	57.6	-77.8	-280
6-Carboxydopamine 3-OH	MP2	-106	-121	-1.12	55.4	-72.5	-266
D86A	M062X	-109	-127	-1.06	56.1	-74.3	-276
6-Carboxydopamine 3-OH	MP2	-110	-123	4.41	-1.60	-86.4	-339
E146A	M062X	-114	-129	0.932	-1.31	-89.5	-354

6-Carboxydopamine 3-OH	MP2	-105	-124	-0.488	-1.06	-82.4	-335
D86A, E146A	M062X	-109	-131	-0.418	-0.798	-85.3	-346
6-Carboxydopamine 4-OH	MP2	-130	-132	-17.6	4.17	-94.2	-397
Wild type	M062X	-135	-138	-21.2	1.97	-98.0	-418
6-Carboxydopamine 4-OH	MP2	-129	-131	0	-0.0957	-93.3	-381
D86A	M062X	-134	-137	0.0861	-3.44	-97.1	-400
6-Carboxydopamine 4-OH	MP2	-123	-130	-6.60	-0.116	-94.8	-377
E146A	M062X	-128	-137	-11.1	0.0114	-98.1	-397
6-Carboxydopamine 4-OH	MP2	-116	-130	-0.317	-0.137	-89.8	-358
D86A, E146	M062X	-120	-136	-0.138	-0.0153	-92.5	-373
6-ethenyldopamine 3-OH	MP2	-16.5	34.7	-113	-99.3	39.1	-166
Wild type	M062X	-19.8	32.8	-117	-103	38.8	-178
6-ethenyldopamine 3-OH	MP2	-16.6	34.5	1.42	-104	39.8	-56.4
D86A	M062X	-20.0	39.4	1.69	-109	39.4	-64.6
6-ethenyldopamine 3-OH	MP2	-9.59	-12.2	-18.1	-0.445	-6.42	-56.0
E146A	M062X	-13.1	-14.2	-21.5	-0.235	-6.79	-63.6
6-ethenyldopamine 3-OH	MP2	-17.9	33.1	1.68	-0.722	38.3	41.7
D86A, E146A	M062X	-21.5	31.4	1.96	-0.376	37.9	38.2
6-ethenyldopamine 4-OH	MP2	-65.5	-69.6	-74.9	-20.1	-7.50	-248
Wild type	M062X	-69.8	-75.6	-81.6	-21.6	-7.52	-265
6-ethenyldopamine 4-OH	MP2	-60.6	-71.1	1.67	-20.2	-6.23	-170
D86A	M062X	-64.4	-77.2	1.87	-21.5	-6.65	-180
6-ethenyldopamine 4-OH	MP2	-114	-124	-35.9	-0.662	-55.7	-344
E146A	M062X	-119	-130	-40.2	-0.424	-56.4	-359

6-ethenyldopamine 4-OH	MP2	-61.1	-70.8	1.46	-0.276	-7.16	-151
D86A, E146A	M062X	-64.7	-76.5	1.62	-0.0960	-6.95	-159
Resveratrol 3-OH	MP2	-114	-119	31.2	38.7	-59.1	-239
Wild type	M062X	-118	-125	30.5	39.3	-60.3	-250
Resveratrol 3-OH	MP2	-111	-120	-1.42	31.7	-57.3	-274
D86A	M062X	-116	-126	-1.38	30.5	-58.7	-287
Resveratrol 3-OH	MP2	-110	-120	31.5	-0.517	-69.7	-282
E146A	M062X	-114	-125	30.9	-0.355	-70.6	-293
Resveratrol 3-OH	MP2	-109	-119	-1.39	-0.685	-70.6	-315
D86A, E146A	M062X	-113	-125	-1.31	-0.453	-71.7	-325
Resveratrol 5-OH	MP2	-106	-125	39.5	39.3	-60.2	-230
Wild type	M062X	-109	-132	39.6	39.3	-61.9	-245
Resveratrol 5-OH	MP2	-105	-125	-1.35	39.4	-60.2	-271
D86A	M062X	-109	-132	-1.33	39.3	-61.9	-286
Resveratrol 5-OH	MP2	-106	-124	39.1	-0.558	-60.2	-270
E146A	M062X	-110	-130	39.2	-0.346	-62.2	-284
Resveratrol 5-OH	MP2	-106	-123	-1.31	-0.56	-60.1	-310
D86A, E146A	M062X	-110	-130	-1.30	-0.347	-62.2	-325